

Validating Quantum State Preparation Programs

Liyi Li¹[0000-0001-8184-0244], Anshu Sharma²[0000-0002-8686-5835],
Zoukarneini Difaizi Tagba¹, Sean Frett¹[0009-0004-1671-9578], and Alex
Potanin³[0000-0002-4242-2725]

¹ Iowa State University, USA
{liyili2,difaizi,fretts}@iastate.edu

² The College of William and Mary, USA
agsharma@wm.edu

³ Australian National University, Australia
alex.potanin@anu.edu.au

Abstract. One of the key steps in quantum algorithms is to prepare an initial quantum superposition state with distinct features. These *state preparation* algorithms are essential to the behavior of quantum algorithms, and complicated state preparation algorithms are difficult to program correctly and effectively. We present QSV: a high-assurance framework implemented with the Rocq proof assistant, permitting the development of quantum state preparation programs and validating them to correctly reflect quantum program behaviors. The key is to reduce the program correctness assurance for a program containing a quantum superposition state to that of the program state without superposition. The reduction enables the development of *an effective framework for validating quantum state preparation algorithm implementations on a classical computer* — a problem considered hard and without a clear solution until now. We utilize the QuickChick property-based testing framework to validate state preparation programs. We evaluated the effectiveness of our approach across 5 case studies implemented using QSV; these cases are not simulatable on current quantum simulators.

Keywords: Quantum Computing · Property-based Testing

1 Introduction

Despite recent advances [40,55,53,23,35,52], quantum program developers still lack tools to quickly validate program correctness—testing a program with many test inputs in a short time—and other properties when writing comprehensive programs [24,51]. Testing quantum programs directly on quantum hardware is problematic because running actual quantum computers is expensive, and the probabilistic nature of quantum computing means repeated trials may be necessary to validate correctness, driving up costs further. Ideally, we should ensure

that a program satisfies user specifications before running it on the hardware. Unfortunately, such a framework might not exist for validating a quantum program for arbitrary properties since quantum programs are not classically simulatable by naive state-vector simulation without an exponential number of classical bits relative to qubits.

A quantum validation framework needs to satisfy three key design goals.

- Programmers can develop a quantum program based on a proper abstraction, with respect to high-level program properties, without worrying too much about low-level gates.
- The framework contains a scalable and effective validator to quickly judge the correctness of a user-defined program, as well as other properties, based on certain types of quantum program patterns.
- The validated program can be compiled into a quantum circuit for execution.

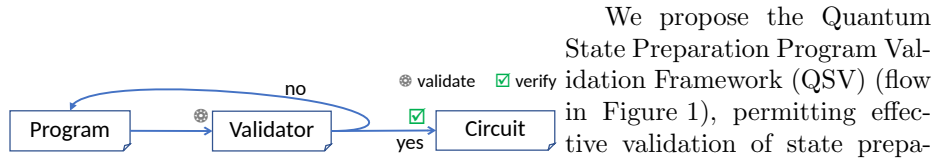


Fig. 1: The QSV Flow

We propose the Quantum State Preparation Program Validation Framework (QSV) (flow in Figure 1), permitting effective validation of state preparation programs. *The limitation is discussed in Section 8.* It includes three components. The first is the language, PQASM,

which extends OQASM (Oracle Quantum Assembly Language); the P in PQASM stands for Preparation. To avoid bugs in common libraries [40] and to avoid using operators outside cases they’re specific to (sometimes, there is no documentation to tell what cases they allow), we chose to implement our own operators in PQASM. Users can develop their programs in the PQASM language, enabling them to write state-preparation programs at a high level of abstraction. Such programs can be validated by our validator (the second component), based on QuickChick [43] (a Rocq property-based testing facility), and we show several quantum program patterns effectively validated via our framework. Once a program is adequately developed in QSV, users can use our certified circuit compiler to compile it into a quantum circuit that runs on quantum hardware.

Motivating Examples. Below is a simple state preparation subroutine, preparing a superposition of n distinct basis-ket states, appearing in many algorithms [3,39]. It has the following program transition property (a pre-state is transitioned to a post-state connected by \rightarrow) with program input of a length m qubit array, initialized as $|0\rangle_m$, and output a superposition of n different basis-ket states, each with basis-vector $|k\rangle_m$.

$$|0\rangle_m \rightarrow \sum_{j=0}^{n-1} \frac{1}{\sqrt{n}} |j\rangle_m$$

A state preparation program can be defined as the starting component of a quantum algorithm, typically starting with a length m qubit array, each qubit

initialized as zero ($|0\rangle_m$) state, and preparing a superposition state $\sum_j \alpha_j |c_j\rangle_m$ — a linear sum of pairs (basis-kets) of complex amplitude α_j and bitstring (basis-vector) c_j such that $\sum_j |\alpha_j|^2 = 1$ — via a series of quantum operations.

Superposition is a key feature of quantum states, and quantum computers can execute programs with superposition states to query all possible inputs simultaneously, as discussed in Section 2. Many quantum algorithms require a comprehensive design of state preparation components with different superposition structures, e.g., the n basis-ket state in Figure 2b.

A difficulty in developing these programs is that quantum program operations might affect every basis-ket in a superposition that might contain exponentially many basis-ket states, unlike the classical programs, where only a single basis-ket might be affected. In Figure 2a, a function f is applied to every basis-ket in the quantum superposition state after all Hadamard operations were applied. Moreover, many quantum languages are circuit-based [4,15,22,21]. These hinder the quantum program development as writing programs becomes unintuitive.

Figure 2b shows a one-step procedure of the repeat-until-success program implementation for the n basis-ket program. The procedure starts with a series of Hadamard operations to prepare a uniform superposition of 2^m basis-kets as $\frac{1}{\sqrt{2^m}} \sum_{j=0}^{2^m-1} |j\rangle_m$, and then compares each basis-ket with the number n ; such a comparison result is stored in the y qubit. If measuring y results in 1, all the basis-kets ($\alpha_j |j\rangle_m$), with bitstring numbers $j \geq n$, disappear, while those bitstrings $j < n$ will stay in x 's quantum state; thus, the correct state is prepared. Since the measurement result 1 is probabilistic, the repeat-until-success program requires repeating the one-step procedure many times to probabilistically prepare the target state. In writing the program, a key component is the comparator ($x < n$) $\otimes y$, comparing every basis-vector of a quantum array x with n and storing the result in qubit y . Such arithmetic operations have effective implementations [32] and circuit-level optimizations [28,56]. Therefore, QSV abstracts all these quantum arithmetic operations and relieves the pain of writing quantum programs. The QSV compiler compiles and optimizes the arithmetic operations to quantum circuits. Moreover, we also provide types to classify different program patterns for users to write state preparation programs.

Even if we permit high-level abstractions in QSV, validating a program might still be challenging because the number of basis-kets in a quantum state increases exponentially with the number of qubits, e.g., with m qubits, the output state $\sum_{j=0}^{n-1} \frac{1}{\sqrt{n}} |j\rangle_m$ might contain any of 2^m basis-kets and checking them individually might be challenging. In developing our validator, we have two observations on quantum algorithms. First, almost all quantum algorithms start with m Hadamard operations to prepare a uniform superposition having 2^m basis-kets. These beginning Hadamard operations are simple enough and do not need to be validated, but they provide the source of a superposition state for later program operations to carve on. Second, even though quantum operations are probabilistic, one can "determinize" their behaviors. If we consider the superposition of basis-kets as an array of basis-kets, quantum operations, except measurement, behave similarly to higher-order map functions applying to the quantum state.

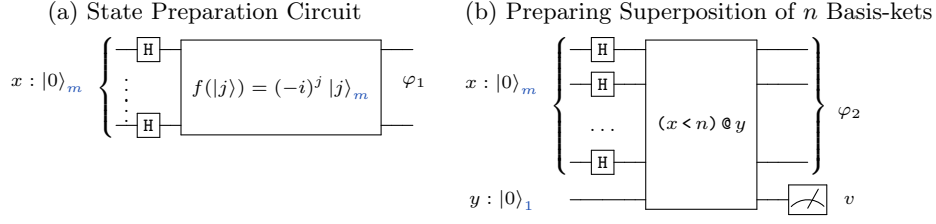


Fig. 2: x has m qubits, and y has 1 qubit; $\varphi_1 = \sum_{j=0}^{2^m-1} (-i)^j |j\rangle_m$. The @ symbol indicates in what qubit the result of an operation is stored. The right is one step in the repeat-until-success program to prepare the superposition state. $\varphi_2 = \frac{1}{\sqrt{n}} \sum_{j=0}^n |j\rangle_m$ if $v = 1$; otherwise, $\varphi_2 = \frac{1}{\sqrt{2^m-n}} \sum_{j=n}^{2^m} |j\rangle_m$.

Measurement behaves similarly to a set selection, selecting a basis-ket element in the array, and the probability of such selection can be computed based on the amplitude value associated with the basis-ket.

QSV classifies beginning Hadamard operations as a special `Had` type, to indicate that they are the source of the superposition state. When testing, instead of faithfully representing their operational behavior, QSV adopts a random pick of an individual basis-ket state as a representative, and validates programs based on transitions of the basis-ket. A measurement operation is then determinized and its probability is simply calculated via the amplitude value in the basis-ket.

For example, in dealing with the n basis-ket program above, after applying the Hadamard operations, the program property is turned as the one on the left below, where $\sum_{j=0}^{2^m-1} \frac{1}{\sqrt{2^m}} |j\rangle_m$ being the result of applying m Hadamard operations. The QSV process of determinizing the basis-kets is to select a particular j , which turns the program property to be the right one.

$$\sum_{j=0}^{2^m-1} \frac{1}{\sqrt{2^m}} |j\rangle_m \rightarrow \sum_{j=0}^{n-1} \frac{1}{\sqrt{n}} |j\rangle_m \quad \forall j \in [0, 2^m), \frac{1}{\sqrt{2^m}} |j\rangle_m \rightarrow \left(\frac{1}{\sqrt{n}} |j\rangle_m \wedge j \in [0, n)\right)$$

Essentially, the validation process based on the right property is to assume a single basis-ket $\frac{1}{\sqrt{2^m}} |j\rangle_m$ with a bitstring $j \in [0, 2^m)$, then to validate to see if the output is the bitstring j within range of $[0, n)$ and the associated amplitude being $\frac{1}{\sqrt{n}}$. Via a property-based testing facility, such as QuickChick, by testing the program with enough candidate basis-kets, it will be highly likely that our validator can capture a bug if there is any. After validation, we compile the program to a quantum circuit via our certified compiler.

Contributions and Roadmap. We present QSV, enabling programmers to develop state-preparation programs. Our contributions are as follows, with all Rocq proofs and experiment results available. Limitations are in Section 8.

- We present the syntax, semantics, and type system of PQASM, allowing users to define programs with a type-soundness proof in Rocq (Section 3).

- We develop a property-based testing (PBT) framework for validating programs written in PQASM (Section 4) by showing a general flow of constructing such PBT frameworks for validating quantum programs.
- We certify a compiler from PQASM to SQIR [28] (Section 4.2) to ensure that our PQASM tool correctly reflect quantum program behaviors.
- We evaluate PQASM via a selection of state preparation programs and demonstrate that QSV is capable of validating the programs (Sections 5 and 6), which are hard to verify or validate if the input qubit length is normal (60 qubits per register and up to 361 qubits as the total input qubit size), based on the Qiskit quantum simulator and DDSim [14].

2 Background on Quantum Computing

Quantum Data and Computation. A quantum datum consists of one or more qubits. A single qubit can be represented as a two-dimensional vector $\begin{pmatrix} z_1 \\ z_2 \end{pmatrix}$, where z_1 and z_2 are complex amplitudes with $|z_1|^2 + |z_2|^2 = 1$. Using Dirac notation, this is written as $z_1|0\rangle + z_2|1\rangle$, with $|0\rangle$ and $|1\rangle$ as the *computational basis-vectors*. When both z_1 and z_2 are non-zero, the qubit is in a superposition of the kets $|0\rangle$ and $|1\rangle$. The value inside the ket is a possible measurement outcome, and the norm square of the scalar factor, e.g., $|z_1|^2$ and $|z_2|^2$, is the probability of the measurement outcome. Multi-qubit data is constructed via the tensor product, e.g., $|0\rangle \otimes |1\rangle = |01\rangle$. However, not all multi-qubit states can be separated into tensor products; some are entangled states, such as the Bell pair $\frac{1}{\sqrt{2}}(|00\rangle + |11\rangle)$.

Quantum computation applies unitary gates to evolve the state of qubits. A gate is represented by a unitary matrix U that acts on the qubit state vector $|\psi\rangle$, producing a new state $U|\psi\rangle$, e.g., the Hadamard gate $H = \frac{1}{\sqrt{2}}\begin{pmatrix} 1 & 1 \\ 1 & -1 \end{pmatrix}$ transforms computational basis states into superpositions: applying H to $|0\rangle$ yields $|+\rangle = \frac{1}{\sqrt{2}}(|0\rangle + |1\rangle)$, and applying H to $|1\rangle$ yields $|-\rangle = \frac{1}{\sqrt{2}}(|0\rangle - |1\rangle)$. These operations are composed in quantum circuits for computations, where each wire denotes a qubit and each gate denotes a transformation applied at a specific time.

Measurement collapses the quantum state to a classical outcome with a probability determined by the amplitudes. For instance, measuring $\frac{1}{\sqrt{2}}(|0\rangle + |1\rangle)$ yields $|0\rangle$ or $|1\rangle$, each with probability $\frac{1}{2}$. After measurement, the state irreversibly collapses to the observed basis state, and quantum coherence is lost.

Quantum Oracles. Quantum algorithms manipulate input information encoded in “oracles”, which are callable black-box circuits. Quantum oracles are usually quantum-reversible implementations of classical operations, especially arithmetic operations. Their behavior is defined in terms of transitions between single basis-kets. We can infer the global state behavior based on the single basis-ket behavior through the quantum summation formula below. This resembles an array map operation in Figure 2a. OQASM in VQO [32] is a language that permits the definitions of quantum oracles with efficient verification and testing facilities by viewing quantum oracle operations as aggregate operations.

Repeat-Until-Success Quantum Programs. A repeat-until-success program utilizes the probabilistic feature of partial measurement operations. It first sets

up a one-step repeat-until-success by linking the desired quantum state with the success measurement of a certain classical value. If such a value is observed after measurement, the desired state is successfully prepared; otherwise, we repeat the one-step procedure. One such example procedure is in Figure 2b to repeat the n basis-ket superposition state. If we measure out $v = 1$, the desired state φ is prepared; otherwise, we repeat the procedure.

No Cloning Theorem indicates there exists no general way of exactly copying a quantum datum [54]. In quantum circuits, it relates to ensuring the reversibility of unitary gate applications. For example, the controlled node and controlled body of a quantum control gate cannot refer to the same qubits, e.g., $\text{CU } q \ \iota$ violates the property if q is mentioned in ι . PQASM enforces no cloning by typing.

3 PQASM: A Language for Quantum State Preparations

We designed PQASM to express quantum-state preparation programs at a high-level abstraction. PQASM operations leverage a quantum-state design, with a type system to track the types of different qubits. Such types restrict the kinds of quantum states, facilitating effective validation and analysis of the PQASM program utilizing our quantum state representations. This section presents PQASM states and the language’s syntax, semantics, typing, and soundness results. More semantic and typing rules are in Section A.

As a running example, we program the n basis-ket state preparation in Definition 1 (figures in Figure 2b). The repeat-until-success program creates an qubit array \bar{q} consisting of all zeroes and a new qubit q' , applies a Hadamard gate to each qubit in \bar{q} , uses a comparison operator $(\bar{q} < n) @ q'$ comparing \bar{q} with n and storing the result in q' , measures the qubit q' , and repeats the process until the measurement result is 1. $\mathbb{H}(\bar{q})$ is a syntactic sugar meaning $\mathbb{H}(\bar{q}[0]) ; \dots ; \mathbb{H}(\bar{q}[m-1])$.

Definition 1 (Example Pqasm program P to prepare n superposition states in \bar{q}). Qubit array length is at least $\log(n) + 1$; q' is a single qubit.

$P \triangleq \text{new}(\bar{q}) ; \text{new}(q') ; \mathbb{H}(\bar{q}) ; (\bar{q} < n) @ q' ; \text{let } x = \mathcal{M}(q') \text{ in if } (x = 1) \{ \} \text{ else } P$

3.1 Pqasm States and Syntax

A PQASM program state Φ is represented based on the grammar in Figure 3, mapping from qubit records θ to a quantum datum φ . A quantum datum is managed as qubit records, each of which is a collection of qubits possibly being entangled, while qubits in different records are guaranteed to have no entanglement. Our quantum data consist of a quantum entanglement state that can be analyzed as two portions: 1) a sequence of sum operators $\sum_{b_1=0}^1 \dots \sum_{b_n=0}^1$, and 2) a basis-ket ρ , a pair of a complex amplitude z and a tensor product of basis vector η , which is a tensor of single qubit basis states ν . Each sum operator represents the creation of a superposition state via a Hadamard operation \mathbb{H} , i.e., the number of sum operators in a state represents the number of Hadamard operations applied to qubits in the state so far. The variable $\rho = z \cdot \eta$ represents a

Qubit Name	q	Nat	$n, m \in \mathbb{N}$	Real	$r \in \mathbb{R}$
Complex	$z \in \mathbb{C}$	Bit	$b \in \{0, 1\}$	Bitstring	$c ::= \bar{b}$
Qubit Basis State	$\nu ::= b\rangle_1$				$ \Delta(r)\rangle$
Qubit Records	$\theta ::= (\bar{q}_1, \bar{q}_2, \bar{q}_3)$				
Type	$\tau ::= \mathbf{Had} \mid \mathbf{Nor} \mid \mathbf{Rot}$				
Basis Vector	$\eta ::= \otimes_j \nu_j$				
Basis-Ket	$\rho ::= z \cdot \eta$				
Quantum Data	$\varphi ::= \rho \mid \sum_{b=0}^1 \varphi$				
Quantum State	$\Phi ::= \theta \rightarrow \varphi$				

Fig. 3: State syntax. \bar{S} : a sequence of S . $|c\rangle_{n+1} \equiv |c[0]\rangle_1 \otimes \dots \otimes |c[n]\rangle_1$, as $|c| = n+1$.

Classical Variable	x, y	Boolean Expressions	B
Parameters	$\alpha ::= \bar{q} \mid n$		
OQASM Arith Ops	$\mu ::= \mathbf{add}(\alpha, \alpha) \mid (n * \alpha) \% m \mid (\alpha = \alpha) @ q \mid (\alpha < \alpha) @ q \mid \dots$		
Instruction	$\iota ::= \mu \mid \mathbf{Ry}^r q \mid \mathbf{CU} q \iota \mid \iota ; \iota$		
Program	$e ::= \iota \mid e ; e \mid \mathbf{H}(q) \mid \mathbf{new}(q) \mid \mathbf{let} x = \mathcal{M}(\bar{q}) \mathbf{in} e \mid \mathbf{if} (B) e \mathbf{else} e$		

Fig. 4: PQASM syntax.

basis-ket of a quantum state. To understand the relation between a basis-ket and a quantum superposition state as a linear sum, one can think of a superposition state as a collection of "quantum choices", and a basis-ket represents a possible choice, i.e., a measurement of a qubit record produces one possible choice, with the amplitude z related to the probability of the choice.

A qubit basis state ν has one of two forms, $|b\rangle_1$ and $|\Delta(r)\rangle$. The former corresponds to the **Had** and **Nor** types and the latter corresponds to the **Rot** type. The three types of qubit basis states are represented as the three fields in a qubit record, i.e., $(\bar{q}_1, \bar{q}_2, \bar{q}_3)$ has three disjoint qubit sequences. \bar{q}_1 is always typed as **Had**, \bar{q}_2 has type **Nor**, and \bar{q}_3 has type **Rot**. The **Had** and **Nor** typed qubits are in the computational basis. The **Rot** typed basis state is different from the other types in terms of *bases*, and it has the form $|\Delta(r)\rangle = \cos(r)|0\rangle_1 + \sin(r)|1\rangle_1$, which is a basis state in the Y -rotated Hadamard basis. Applying a **Ry** with the Y -axis angle r to a $|0\rangle_1$ qubit results in $|\Delta(r)\rangle = \cos(r)|0\rangle + \sin(r)|1\rangle$.

Figure 4 presents PQASM's syntax. A PQASM program e is either an instruction ι , a sequence operation $e ; e$, applying a Hadamard operation $\mathbf{H}(q)$ to a qubit q to create a superposition, creating (**new**(q)) a new blank qubit q , a **let** binding that measures a sequence of qubits \bar{q} and uses the result x in e , or classical conditional **if** (B) e **else** e with classical Boolean guard B . Each **let** binding assigns a measurement result of qubits \bar{q} to a variable x , representing a binary sequence. We assume $\mathbf{H}(\bar{q})$ and **new**(\bar{q}) as syntactic sugars of applying a sequence of Hadamard and new-qubit operations.

The instructions ι correspond to unitary quantum circuit operations, including oracle arithmetic operations (μ) implementable through OQASM operations [32] on a qubit sequence \bar{q} (detailed in Section C), a Y -axis rotation gate $\mathbf{Ry}^r q$

$$\begin{aligned}
\llbracket \mu \rrbracket \eta &= \eta[q \mapsto \llbracket \mu \rrbracket \eta(\bar{q})] && \text{where } FV(\mu) = \bar{q} \\
\llbracket \text{Ry}^r q \rrbracket \eta &= \eta[q \mapsto |\Delta(r)\rangle] && \text{where } \eta(q) = |0\rangle_1 \\
\llbracket \text{Ry}^r q \rrbracket \eta &= \eta[q \mapsto |\Delta(\frac{3\pi}{2} - r)\rangle] && \text{where } \eta(q) = |1\rangle_1 \\
\llbracket \text{Ry}^r q \rrbracket \eta &= \eta[q \mapsto |\Delta(r + r')\rangle] && \text{where } \eta(q) = |\Delta(r')\rangle \\
\llbracket \text{CU } q \ \iota \rrbracket \eta &= \text{cu}(\eta(q), \iota, \eta) && \text{where } \text{cu}(|0\rangle, \iota, \eta) = \eta \quad \text{cu}(|1\rangle, \iota, \eta) = \llbracket \iota \rrbracket \eta \\
\llbracket \iota_1; \iota_2 \rrbracket \eta &= \llbracket \iota_2 \rrbracket (\llbracket \iota_1 \rrbracket \eta)
\end{aligned}$$

$$\eta[\bar{q} \mapsto \eta'] = \eta[\forall q \in \bar{q}. q \mapsto \eta'(q)]$$

Fig. 5: Instruction level PQASM semantics; $\eta(\bar{q})$: the states of the qubits \bar{q} in η .

that rotates an angle r , a quantum control instruction ($\text{CU } q \ \iota$), and a sequence operation ($\iota ; \iota$). Operation $\text{CU } q \ \iota$ applies instruction ι *controlled* on qubit q . In this paper, we provide several sample arithmetic oracle operations μ in Figure 4, such as addition ($\text{add}(\alpha, \alpha)$, adding the first to the second), modular multiplication ($(n * \alpha) \% m$), quantum equality ($(\alpha = \alpha) @ q$), quantum comparison ($(\alpha < \alpha) @ q$), etc. Each parameter α is either a group of qubits \bar{q} or a number n . Recall that a basis-ket state of a qubit array \bar{q} is essentially a bitstring with a complex amplitude. A quantum arithmetic operation applies the classical version of the operation to each basis-ket in a quantum superposition state, e.g., $(\bar{q} = n) @ q$ compares the bitstring representation of each basis-ket in \bar{q} with the number n and stores the result in q . In a PQASM program containing qubit array \bar{q} , x in a `let` binding binds a local classical value (x 's value) with the computational basis measurement result (\mathcal{M}) on qubits \bar{q} . While the classical variable scope is local, the quantum qubits are immutable and globally scoped, i.e., quantum operations are applied to a global quantum state; each qubit in the state is referred to by quantum qubit names (q) in the program. In PQASM, we express a `SKIP` operation ($\{\}$) via a μ operation having empty qubits, as $\mu \equiv \{\}$ **when** $FV(\mu) = \emptyset$ (FV collects free variables).

3.2 Semantics

The PQASM semantics has two levels: instruction and program levels. The former is a partial function $\llbracket - \rrbracket$ from an instruction ι and input basis vector state ρ to an output state η' , written $\llbracket \iota \rrbracket \eta = \eta'$, shown in Figure 5. The *program* level semantics is a labelled transition system $(\Phi, e) \xrightarrow{r} (\Phi', e')$ in Figure 6, stating that the input configuration (Φ, e) is possibly evaluated to an output configuration (Φ', e') with the probability r . It essentially represents a Markov chain, where a program evaluation path is a chain of probabilities that shows the probability of reaching a particular configuration from the initial configuration.

The instruction level semantic rules assume that one can locate the state of a qubit q in η as $\eta(q)$, where we can refer to $\eta[q \mapsto \nu]$ as updating the qubit state ν for the qubit q in η . Recall that a length n basis vector state η is a tuple of n qubit values, modeling the tensor product $\nu_1 \otimes \dots \otimes \nu_n$. The rules implicitly

$$\begin{array}{c}
 \text{S-INS} \\
 b = b_1, \dots, b_n \quad \varphi = \sum_{b_1=0}^1 \dots \sum_{b_n=0}^1 z_b \cdot \eta_b \quad \llbracket \iota \rrbracket(\eta_b) = \eta'_b \quad \text{S-NEW} \\
 \hline
 (\Phi[\theta \mapsto \varphi], \iota) \xrightarrow{1} (\Phi[\theta \mapsto \sum_{b_1=0}^1 \dots \sum_{b_n=0}^1 z_b \cdot \eta'_b], \{\}) \quad (\Phi, \text{new}(q)) \xrightarrow{1} (\Phi[(\emptyset, q, \emptyset) \mapsto |0\rangle_1], \{\}) \\
 \\
 \text{S-HAD} \\
 \hline
 (\Phi[(\emptyset, q, \emptyset) \mapsto |b\rangle_1], \mathbf{H}(q)) \xrightarrow{1} (\Phi[(q, \emptyset, \emptyset) \mapsto \sum_{j=0}^1 (-1)^{j \cdot b} |j\rangle_m], \{\}) \\
 \\
 \text{S-MEA} \\
 \Phi = \Phi' \uplus \{(\uparrow \bar{q} \mapsto \sum_j z_j |c\rangle_m |c_j\rangle_n + \phi(\bar{q}', c \neq \bar{q}'))\} \quad r = \sum_j |z_j|^2 \\
 \hline
 (\Phi, \text{let } x = \mathcal{M}(\bar{q}) \text{ in } e) \xrightarrow{r} (\Phi' \uplus \{(\uparrow \bar{q})n\bar{q} : \sum_j \frac{z_j}{\sqrt{r}} |c_j\rangle_m\}, e[c/x]) \\
 \\
 \uparrow \bar{q} \triangleq \exists \bar{q}_1, \bar{q}_2, \bar{q}_3. \uparrow \bar{q} = (\bar{q}_1, \bar{q}_2, \bar{q}_3) \wedge \bar{q} \subseteq \bar{q}_1 \uplus \bar{q}_2 \uplus \bar{q}_3 \\
 (\sum_i z_i |c_i\rangle_m |c'_i\rangle_n + \varphi)\langle \bar{q}, b \rangle \triangleq \sum_i z_i |c_i\rangle_m |c'_i\rangle_n \quad \text{where } \forall i. |c_i| = |\bar{q}'| = m \wedge \llbracket b[c_i/\bar{q}'] \rrbracket = \text{true}
 \end{array}$$

Fig. 6: Selected program Level PQASM rules.

map each qubit q to a state, e.g., $\eta(q)$ corresponds to some sub-state ν_q , where ν_q locates at the q 's position in η . Many of the rules in Figure 5 update a *portion* of a state. We write $\eta[q \mapsto \nu_q]$ to update the state of the qubit of q in η with ν_q , and $\eta[\bar{q} \mapsto \eta']$ to update a range of qubits \bar{q} according to the vector state η' , i.e., we update each $q \in \bar{q}$ with the qubit value $\eta'(q)$ and $|\eta'| = |\bar{q}|$. The function cu is a conditional operation depending on the **Nor**/**Had** typed qubit q .

Figure 6 shows selected program-level semantic rules. Since qubit records in a program state Φ partition the qubit domain, we can think of Φ as a multiset of pairs of qubit records and state values, as in S-MEA, i.e., $\Phi[\theta \mapsto \varphi] \equiv \Phi \uplus \{\theta \mapsto \varphi\}$. Rule S-INS connects the instruction level semantics with the program level by evaluating each basis vector state η through the instruction ι . Rule S-NEW creates a new blank ($|0\rangle_1$) qubit, which is stored in the record $(\emptyset, q, \emptyset)$, a qubit (q) being created are **Nor** typed. For a **Nor** typed qubit $(\emptyset, q, \emptyset)$, rule S-HAD turns the qubit to be **Had** typed superposition, as $(q, \emptyset, \emptyset)$. The measurement rule (S-MEA) produces a probability r label, and the value comes from the measurement result. We first rewrite the quantum state to be a linear sum of computational basis-kets $\sum_j r_j |c\rangle_m |c_j\rangle_n + \varphi(\bar{q}', c \neq \bar{q}')$, where every basis-vector $|c\rangle_m$ (or $|c_j\rangle_n$) is a bitstring, and all the sum operators are resolved as a single sum.

Any PQASM state can be written as a sum of computational basis-kets. As the equations shown below, the basis-ket state $|c\rangle_n |\Delta(r)\rangle$ can be rewritten to be a sum of two computational basis-kets as $\cos(r) |c\rangle_n |0\rangle_1 + \sin(r) |c\rangle_n |1\rangle_1$, while the two sum operators can be replaced as a single sum operator over length-2 bitstring c , where we replace b_j with $c[0]$ (indexing 0 of c) and b_k with $c[1]$.

$$|c\rangle_n |\Delta(r)\rangle \equiv \cos(r) |c\rangle_n |0\rangle_1 + \sin(r) |c\rangle_n |1\rangle_1 \quad \sum_{b_j=0}^1 \sum_{b_k=0}^1 \eta \equiv \sum_{c \in \{0,1\}^2} \eta[c[0]/b_j][c[1]/b_k]$$

$$\begin{array}{c}
\text{RyN} \\
\frac{}{\{(\emptyset, \{q\}, \emptyset)\} \uplus \Omega \vdash_{\text{c}} \text{Ry}^r q \triangleright \{(\emptyset, \emptyset, \{q\})\} \uplus \Omega} \\
\\
\text{RyH} \quad \frac{\text{Rot}(\theta) = \{q\} \uplus \bar{q}}{\{\theta\} \uplus \Omega \vdash_g \text{Ry}^r q \triangleright \{\theta\} \uplus \Omega} \quad \text{EQV} \quad \frac{\Omega \equiv \Omega'}{\Omega' \vdash_g e \triangleright \Omega''} \quad \text{TUP} \quad \frac{\Omega \vdash_{\text{c}} \iota \triangleright \Omega'}{\Sigma; \Omega \vdash \iota \triangleright \Omega'} \quad \text{NEW} \quad \frac{q \notin \Omega}{\Sigma; \Omega \vdash \text{new}(q) \triangleright \Omega \uplus \{(\emptyset, q, \emptyset)\}} \\
\\
\text{CuN} \quad \frac{\{\text{Nor}(\theta) \downarrow \bar{q}\} \uplus \Omega \vdash_{\text{M}} \iota \triangleright \{\text{Nor}(\theta) \downarrow \bar{q}\} \uplus \Omega}{\{\text{Nor}(\theta) \downarrow \{q\} \uplus \bar{q}\} \uplus \Omega \vdash_g \text{CU } q \iota \triangleright \{\text{Nor}(\theta) \downarrow \{q\} \uplus \bar{q}\} \uplus \Omega} \quad \text{HT} \quad \frac{}{\Sigma; \Omega \uplus \{(\emptyset, q, \emptyset)\} \vdash \text{H}(q) \triangleright \Omega \uplus \{(\emptyset, \emptyset, \emptyset)\}} \\
\\
\text{CuH} \quad \frac{\{\text{Had}(\theta) \downarrow \bar{q}\} \uplus \Omega \vdash_{\text{M}} \iota \triangleright \{\text{Had}(\theta) \downarrow \bar{q}\} \uplus \Omega}{\{\text{Had}(\theta) \downarrow \{q\} \uplus \bar{q}\} \uplus \Omega \vdash_g \text{CU } q \iota \triangleright \{\text{Had}(\theta) \downarrow \{q\} \uplus \bar{q}\} \uplus \Omega} \quad \text{MEA} \quad \frac{\bar{q} \subseteq \theta \quad \Sigma \cup \{x\}; \Omega \uplus \{\theta n \bar{q}\} \vdash e \triangleright \Omega'}{\Sigma; \Omega \uplus \{\theta\} \vdash \text{let } x = \mathcal{M}(\bar{q}) \text{ in } e \triangleright \Omega'}
\end{array}$$

Fig. 7: Selected type rules. $(\bar{q}_1, \bar{q}_2, \bar{q}_3) \setminus \bar{q} \triangleq (\bar{q}_1 \setminus \bar{q}, \bar{q}_2 \setminus \bar{q}, \bar{q}_3 \setminus \bar{q})$; $\bar{q}_1 \setminus \bar{q}$: set subtract.

3.3 Typing

In PQASM, typing is with respect to a *type environment* Ω , a set of qubit records partitioning qubits into different disjoint union regions, and a *kind environment* Σ , a set tracking local variable scopes. Typing judgments are two leveled, and are written as $\Omega \vdash \iota \triangleright_g \Omega'$ and $\Sigma; \Omega \vdash e \triangleright \Omega'$, which state that instruction ι and program expression e are well-typed under Ω and Σ , and transforms variables' bases as characterized by Ω' . Ω is populated via qubit creation operations (**new**), while Σ is populated via **let** binding. Selected typing rules are in Figure 7.

The instruction level type system is flow-sensitive, where g is the context flag and can be either **M** or **C**, indicating whether the current instruction is inside a controlled operation. The program level type system communicates with the instruction level by assuming a **C** mode context flag, shown in rule **TUP**. We explain the necessity of the context flag below. Each qubit record θ represents an entanglement group, i.e., qubits in the same record might or might not be entangled, while qubits in different records are ensured not to be entangled.

$$\begin{aligned}
(\bar{q}_1, \bar{q}_2, \bar{q}_3) \uplus (\bar{q}_4, \bar{q}_5, \bar{q}_6) &\equiv (\bar{q}_1 \uplus \bar{q}_4, \bar{q}_2 \uplus \bar{q}_5, \bar{q}_3 \uplus \bar{q}_6) \\
(\emptyset, \bar{q}_1 \uplus \bar{q}_2, \bar{q}_3 \uplus \bar{q}_4) &\equiv (\emptyset, \bar{q}_1, \bar{q}_3) \uplus (\emptyset, \bar{q}_2, \bar{q}_4)
\end{aligned}$$

In our type system, we permit ordered equational rewrites among quantum qubit states. Each type environment, mainly the operation \uplus , admits associativity, commutativity, and identity equational properties. The \uplus operations in the three fields in a qubit record also admit the three properties. Other than the three equational properties, we admit the above partial order relations, where we permit the rewrites from left to right in our type system to permit qubit records merging and splitting. Record merging can always happen, i.e., two qubit entanglement groups can be merged into one. Qubit splitting cannot occur in **Had** typed qubits. A qubit record, including a **Had** typed qubit, represents a quantum entanglement with qubits not separable, while qubits being **Nor** and **Rot** typed

can be split into different records. Rule EQV imposes the equivalence relation to permit the rewrites, only allowing rewrites from left to right, of equivalent qubit records. Note that a type environment determines qubit record scopes in a quantum state φ (Figure 3), i.e., a quantum state should have the same qubit record domain as the type environment at a program point, so the equational rewrite of a type environment might affect the qubit state representation.

Other than the equational rewrites, the type system enforces three properties. First, it enforces that classical and quantum variables are properly scoped. Rule MEA includes the local variable x in Σ . Rule NEW creates a new record $(\emptyset, q, \emptyset)$ in the post-environment, provided that q does not appear in any record in Ω . In rule RYH, the premise $\text{Rot}(\theta) = \{q\} \uplus \bar{q}$ utilizes **Rot** to find the **Rot** field in the record θ and ensures that q is in the field. In rule CUH, the premise $\text{Had}(\theta) \downarrow \{q\} \uplus \bar{q}$ ensures that the controlled position q is in the **Had** field in θ . In rule MUT, we ensure that the qubits \bar{q} being applied by the μ operation are **Nor** and **Had** typed, through the premise $\bar{q} \subseteq \bar{q}_1 \cup \bar{q}_2$.

Second, we ensure that expressions and instructions are well-formed, i.e., any control qubit is distinct from the target(s), which enforces the quantum *no-cloning rule*. In rules CUH and CUN for control operations, when typing the target instruction ι (the upper level), we remove the control qubit q in the records to ensure that q cannot be mentioned in ι . In rule MEA, we also remove the measured qubits \bar{q} from the record θ .

Third, the type system enforces that expressions and instructions leave affected qubits in a proper type (**Nor**, **Had**, and **Rot**), representing certain forms of qubit states, mentioned in Figure 3; therefore, one can utilize the procedure mentioned in Section 1 to analyze PQASM programs effectively. The key is to utilize the summation formula to reduce the analysis of a general quantum state to that of a quantum state without entanglement. Specifically, the $\text{Ry}^r q$ operation is permitted only if q is of **Nor** type, which is turned to **Rot** type and stays there; μ can be applied to **Nor** typed qubits \bar{q} where $FV(\mu) = \bar{q}$; and a control qubit q in **CU** $q \iota$ can be applied to a **Nor** and **Had** typed qubit.

We ensure type restrictions for qubits via pre- and post-type environments. Rule HT permits the generation of **Had** type qubits, a.k.a. superposition qubits q , provided that q is of **Nor** type and not entangled with other qubits. Once a Hadamard operation is applied, we turn the qubit types to **Had** in the post-type environment, so one cannot apply Hadamard operations again to the qubits. This does not mean that users can only apply Hadamard operations once in PQASM, because combining **X** (our oracle operation) and **Ry** gates can produce a Hadamard gate. We utilize the type information to locate the first appearance of Hadamard operations, identify them as the source of superposition, and apply treatments for them in our validation testing framework; see Section 4.1.

In Rules CUN and CUH, we ensure that the pre- and post-type environments are the same. In **CU** $q \iota$, if ι contains a **Ry** operation, applying to a qubit q , q

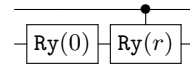


Fig. 8: Ensuring qubits inside a controlled **Ry** have the same type.

must already be **Rot** type. Figure 8 provides a programming prototype satisfying this type requirement, where programmers explicitly add a **Ry** gate before the controlled **Ry** operation to ensure the second qubit is in **Rot** type. The extra **Ry** operation can be a 0 rotation, equivalent to a **SKIP** operation, and can be removed by an optimizer when compiling to quantum circuits. The above qubit type restriction does not depend on the applications of controlled operations. We ensure this by associating the context flags with the instruction level type system. When applying **CU** $q \iota$, rules **CUN** and **CUH** turn the context flag to **M**, indicating that ι lives inside a controlled operation. Rule **RyN** requires a context flag **C**, meaning that the rule is valid only if the **Ry** operation lives outside any controlled operation. In contrast, rule **RyH** does not require a specific context flag, which indicates that a **Ry** operation inside a controlled node must apply to a qubit already in **Rot** type.

Soundness. We prove type soundness: well-typed PQASM programs are well-defined. The type soundness theorem relies on a well-formed definition of a program e , $FV(e) \subseteq \Sigma$, meaning that all free variables in e are bounded by Σ . We also need the definition of the well-formedness of a PQASM state as follows.

Definition 2 (Well-formed state). A state Φ is *well-formed*, $\Omega \vdash \Phi$, iff:

- For every q such that $\Omega(q) = \text{Nor}$ or $\Omega(q) = \text{Had}$, $\Phi(q)$ has the form $|b\rangle_{\mathbf{1}}$.
- For every q such that $\Omega(q) = \text{Rot}$, $\Phi(q)$ has the form $|\Delta(r)\rangle$.

Type soundness is stated as two theorems: type progress and preservation; the proof is by induction on ι and is mechanized in Rocq.

Theorem 1. [PQASM Type Progress] If $\emptyset; \Omega \vdash e \triangleright \Omega'$, $FV(e) \subseteq \emptyset$, and $\Omega \vdash \Phi$, then either $e = \{\}$ or there exists r, e' , and Φ' , such that $(\Phi, e) \xrightarrow{r} (\Phi', e')$.

Proof. Fully mechanized proofs were done by induction on type rules using Rocq.

Theorem 2. [PQASM Type Preservation] If $\Sigma; \Omega \vdash e \triangleright \Omega'$, $FV(e) \subseteq \Sigma$, $\Omega \vdash \Phi$ and $(\Phi, e) \xrightarrow{r} (\Phi', e')$, then there exists Ω_a , such that $\Sigma; \Omega_a \vdash e' \triangleright \Omega'$ and $\Omega_a \vdash \Phi'$.

Proof. Fully mechanized proofs were done by induction on type rules using Rocq.

4 QSV Applications

This section presents QSV applications, based on PQASM programs, to validate and compile the programs, including QSV's PBT (property-based testing) framework and the translation from PQASM to SQIR and proof of its correctness.

4.1 Effectively Validating State Preparation Programs

The QSV validator is built on PBT to ensure that a PQASM program property is correct by attempting to falsify it using thousands of randomly generated input variables. Case studies of our validator are in Section 5. Below, we show its

construction. We leverage the PQASM’s state representation and type system, which ensure that states can be represented effectively, to implement a validation framework for PQASM programs using QuickChick [43], a property-based testing (PBT) framework for Rocq in the style of Haskell’s QuickCheck [20]. The framework has two main utilities: validating PQASM program correctness properties and experimenting with effective implementations. PQASM measurement operations, due to the randomness inherent in quantum measurement, are difficult to test effectively, even with the assistance of program abstractions. To have an effective validation framework, we restrict the properties that can be questioned to solely focus on the properties related to program correctness.

Implementation. PBT randomly generates inputs using a hand-crafted *generator* and confirms that a property holds for these inputs. We develop a validator, based on the methodology in Section 1, using our effective (symbolic) state representation and carefully selecting the properties to validate for a program.

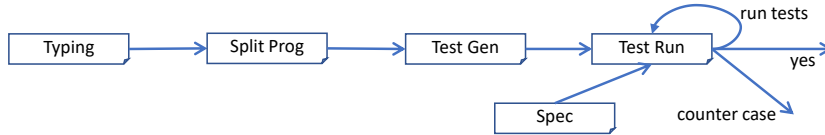


Fig. 9: The Flow of PBT for QSV

Figure 9 shows the flow of the PBT framework. To validate a PQASM program, we first utilize our PQASM type system to generate a type environment Ω for qubits in a program e , i.e., $\emptyset; \emptyset \vdash e \triangleright \Omega$, typing with an empty kind and type environment. Ω partitions all qubits used in e into three sets $(\bar{q}_1, \bar{q}_2, \bar{q}_3)$, with \bar{q}_1 , \bar{q}_2 , and \bar{q}_3 containing all qubits in **Had** type, **Nor** type, and **Rot** type, respectively. In PQASM, once a qubit is assigned to type **Had**, it stays in the type. We utilize the property to locate all **Had** typed qubits in a program e and generate random testing data based on these qubits, i.e., given the set (\bar{q}_1) of **Had** typed qubits in Ω , we generate random boolean values in $\{0, 1\}$ for variables in \bar{q}_1 .

A program is assumed in the form of $e = \mathbf{new}(\bar{q}) ; \mathbf{H}(\bar{q}) ; e'$ ⁴, i.e., all the **new** and **H** operations appear in the front of the program and e' does not contain any such operations. We then split the program by taking the e' part and removing the **new** and **H** operations, assuming they have already been applied. For some program patterns, such as repeat-until-success programs, we replace recursive process variables in e' with $\{\}$ operations so that we only validate one step of a repeat-until-success. While these programs do not have a fixed termination time, QSV focuses on testing a single loop step, as we are not concerned with executing this program but performing property-based testing on it. One example of programming splitting for Definition 1 is given below; it removes the part $\mathbf{new}(\bar{q}) ; \mathbf{new}(q') ; \mathbf{H}(\bar{q})$ and replacing P with $\{\}$.

⁴ $\mathbf{new}(\bar{q})$ and $\mathbf{H}(\bar{q})$ are syntactic sugar for multiple $\mathbf{new}(q)$ and $\mathbf{H}(q)$ operations.

$$P' = (\bar{q} < n) @ q' ; \text{let } x = \mathcal{M}(q') \text{ in if } (x = 1) \{ \} \text{ else } \{ \}$$

The ‘‘Test Gen’’ step in QSV (Figure 9) generates test cases to validate the key component P' above. In Definition 1, after applying the **new** and **H** operations, the post-state is (Φ, P') , with Φ mapping θ , entanglement groups, to superposition states φ . Each **H** operation generates a single qubit uniformly distributed superposition state. However, transitions over a superposition state make it hard to perform effective validation. To resolve this, we treat quantum program operations P' as higher-order map operations and validate the transition correctness based on basis kets, rather than over the whole superposition state.

Generally, given $\theta = (b_0, b_1, \dots, b_m, \bar{q}_2, \bar{q}_3)$, the superposition state φ could also be written in the Dirac notation of $\sum_j \rho_j$ with $\rho_j = z_j \cdot \eta_j$, as follows.

$$\sum_{b_0=0}^1 \sum_{b_1=0}^1 \dots \sum_{b_m=0}^1 z(b_0, b_1, \dots, b_m) \cdot \eta(b_0, b_1, \dots, b_m)$$

Here, b_0, b_1, \dots, b_m are qubit variables assumed to have already been manipulated by the initial **H** operations. Applying a **H** operation to a **Nor** typed qubit $|b_a\rangle_1$ creates a uniformly distributed superposition $\sum_{b=0}^1 \frac{1}{\sqrt{2}} (-1)^{b \cdot b_a} |b\rangle_1$, so it results in the state form above, with $z(b_0, b_1, \dots, b_m)$ and $\eta(b_0, b_1, \dots, b_m)$ being an amplitude and asis-vector formula, respectively. We can then select the symbolic basis-ket state $z(b_0, b_1, \dots, b_m) \cdot \eta(b_0, b_1, \dots, b_m)$ as the representative basis-ket and rewrite φ to be in the form $(\theta \rightarrow z \cdot \eta, P')$, with b_0, b_1, \dots, b_m acting as random variables. For each variable b_j , we can randomly choose the value $b_j \in \{0, 1\}$ for a particular test instance. For m qubits, we have 2^m different instances depending on the different value selection for the random variables.

For P' above, we view each element in the m -qubit array \bar{q} as a random variable. We generate an initial state $(\theta \rightarrow z(\bar{q}[0], \dots, \bar{q}[m-1]) \cdot \eta(\bar{q}[0], \dots, \bar{q}[m-1]), P')$ with $\bar{q}[0], \dots, \bar{q}[m-1]$ being random variables and $\theta = (\bar{q}, q, \emptyset)$. We can then generate test instances for the random variables $\bar{q}[j]$ with $j \in [0, m)$.

As test instances are generated, we can validate the program by running each instance in our PQASM interpreter, based on our program semantics. The interpreter’s result is provided as input to a specification checker to validate whether the specification is satisfied. If the checker makes all test instances return **true**, we validate the program; otherwise, we report a fault. We show below the validation of different program properties.

Validating Correctness. We run a test instance in our interpreter with the initial state, as $(\theta \mapsto z \cdot \eta, P) \longrightarrow^* (\theta' \mapsto z' \cdot \eta', \{ \})$, where $\theta \equiv \theta'$. For a user-specified property ψ , a satisfiability check is applied to $\psi(z \cdot \eta, z' \cdot \eta')$ by replacing variables with $z \cdot \eta$ and $z' \cdot \eta'$. Recall the transformation of correctness property in Section 1 for the program in Definition 1, the key is to conduct validation on individual basis-kets rather than the whole quantum state. Such property transformations can be summarized as the transformation from (1) to (3):

$$(1) \sum_j z_j \cdot \eta_j \rightarrow f(\sum_j z_j \cdot \eta_j) \quad (2) \sum_j z_j \cdot \eta_j \rightarrow \sum_k g(z_k \cdot \eta_k) \wedge \phi(k) \quad (3) \forall j. z_j \cdot \eta_j \rightarrow g'(z_j \cdot \eta_j) \wedge \phi(j)$$

The correctness property should be written in the format of (3). The property (1) describes the program semantics, i.e., f represents the semantic function for

a program e . The effects of such a function can always be in the form of a linear sum by moving the sum operator to the front, as in (2): one can always find g such that $f(\sum_j r_j \cdot \eta_j) = \sum_k g(r_k \cdot \eta_k)$. In some cases, we might need to insert the $\phi(k)$ predicate above, constraining index k in the sum operator. Here, both j and k are indices for two different sum operators. Often, the function g can be turned into an equivalent form g' based on the index j . Note that for certain states, there are properties that hold for the state at large but do not imply that they hold for each term. For instance, when k is a bitstring and $\text{not}(k)$ performs the **not** operator on each value in the bitstring, e.g. $\text{not}(011) = 100$, if $\sum_i |k_i\rangle = \sum_i |\text{not}(k_i)\rangle$ that does not imply that $|k_i\rangle = |\text{not}(k_i)\rangle$.

Once rewriting (1) to (2), we can then transform the formula to (3) without any sum operators, via the axiom of extensionality. Such transformation might come with the index restriction ϕ based on index j , as shown in (3), meaning that we find a representative basis-ket state $r_j \cdot \eta_j$ for the input superposition state and output a basis-ket state $g'(r_j \cdot \eta_j)$, with the index restriction $\phi(j)$.

To validate P' above, we transform the correctness property from the left to the right one below (\Rightarrow is logic implication).

$$x = 1 \Rightarrow \sum_j^{2^m} \frac{1}{\sqrt{2^m}} |j\rangle_m |0\rangle_1 \rightarrow \sum_j^n \frac{1}{\sqrt{n}} |j\rangle_m \quad \forall j \in [0, 2^m]. \quad x = 1 \Rightarrow |j\rangle_m |0\rangle_1 \rightarrow |j\rangle_m \wedge j < n$$

The right property states that, if the measurement results in 1 ($x = 1$), each basis-ket in the pre-state for \bar{q} and q (values $|j\rangle_m$ and $|0\rangle_1$) results in \bar{q} being the same $|j\rangle_m$ with the restriction $j < n$. In implementing a validation property, the flags m and 1 essentially indicate the length of bitstring pieces, cast into a natural number for comparison. To validate the correctness property against P' , we create a length m bitstring for $|j\rangle_m$ and view $j[k]$, for $k \in [0, m)$, being the k -th bit in the bitstring. Recall that P' has an initial basis vector state pattern as $|\bar{q}[0]\rangle_1 \dots |\bar{q}[m-1]\rangle_1 |0\rangle_1$. Here, $|0\rangle_1$ is the state for qubit q and $\bar{q}[0], \dots, \bar{q}[m-1]$ are random variables for qubit array \bar{q} . To check the property, we bind each $j[k]$ with $\bar{q}[k]$ for $k \in [0, m)$, and see if the output basis-ket state results in the same $\bar{q}[0], \dots, \bar{q}[m-1]$. We also check if \bar{q} 's natural number representation is less than n , i.e., we turn $\bar{q}[0], \dots, \bar{q}[m-1]$ to a number and compare it with n .

Validating Other Properties. The above procedure is only useful in validating correctness. There might be other interesting properties, such as probability and effectiveness properties. For example, in validating Definition 1, we might want to ask how likely the qualified state can be prepared, which is hard to validate in general, but it can be effectively sampled out in some cases.

$$x = 1 \Rightarrow \sum_j^{2^m} \frac{1}{\sqrt{2^m}} |j\rangle_m |0\rangle_1 \rightarrow \sum_j^n \frac{1}{\sqrt{n}} |j\rangle_m$$

In the property for P' above, the basis-vector number n is related to \bar{q} 's qubit number m , as $n \in [0, 2^m)$. We explain how to validate the program's effectiveness, i.e., the probability that the repeat-until-success program produces the correct state. Note that superposition states are always uniformly distributed without any Ry operations. The success rate of preparing a superposition state in the repeat-until-success scheme is the ratio between the number of desired basis-vector values ($< n$) and the total number of possible basis-vector values,

i.e., different combinations of $\bar{q}[0], \dots, \bar{q}[m-1]$. We can validate the effectiveness by dividing the number of different desired basis-vectors and the number of possible values in \bar{q} ; that is, 2^m . In general, assume that we have a basis-vector expression $e(\bar{q})$ for m qubits \bar{q} , a measurement statement $\mathcal{M}(e(\bar{q}))$ storing the result in v , and have a boolean check on v as $B(v)$ defining the good states. By assigning $\{0, 1\}^m$ for \bar{q} , the probability of having the good states is the division of number of good state values ($B(e(\bar{q})) = \text{true}$) and the possible basis-vector numbers in $e(\bar{q})$ for all possible assignments. Such a property can be validated by sampling. In some complicated cases, the right property might be hard to validate, but one can always use Rocq to verify the effectiveness via the above scheme.

Performance Optimizations. We took several steps to improve validation performance, e.g., we streamlined the representation of states: per the semantics in Figure 5, in a state with n qubits, the amplitude associated with each qubit can be written as $\Delta(\frac{v}{2^n})$ for some natural number v . Qubit values in both bases are thus pairs of natural numbers: the global phase v (in range $[0, 2^n)$) and b (for $|b\rangle_1$) or y (for $|\Delta(\frac{y}{2^n})\rangle$). A PQASM state φ is a map from qubit positions p to qubit values q ; in our proofs, this map is implemented as a partial function, but for validation, we use an AVL tree (a kind of self-balancing binary tree) implementation (proved equivalent to the functional map). To avoid excessive stack use, we implemented the PQASM semantics function tail-recursively. To run the tests, QuickChick runs OCaml code that it *extracts* from the Rocq definitions; during extraction, we replace natural numbers and operations thereon with machine integers and operations. Performance results are in Section 5.

4.2 Translation from Pqasm to SQIR

We translate PQASM to SQIR by mapping PQASM virtual qubits to SQIR [28], a quantum circuit language based on Rocq, concrete qubit indices, and expanding PQASM instructions to sequences of SQIR gates. To express the classical components of quantum algorithms, SQIR typically utilizes Rocq program constructs. To define our compiler, we use the SQIR one-step nondeterministic semantics, which includes one-step operational semantics for simple Rocq constructs, such as conditionals and classical sequential operations.

Our translation is expressed as the two-level judgments $\Xi \vdash \iota \gg \epsilon$ and $(n, \Xi, e) \gg (n', \Xi', \chi)$, where ϵ is the output SQIR circuit, and Ξ and Ξ' map a PQASM qubit q to a SQIR concrete qubit index (i.e., offset into a global qubit register), χ is a hybrid program including SQIR quantum circuits and Rocq classical programs, and n and n' are the qubit sizes in the whole system.

$$\begin{array}{c} \text{CRy} \\ \hline \Xi \vdash \text{Ry}^r q \gg (\gamma, \text{Ry}^r(\Xi(q))) \end{array} \quad \begin{array}{c} \text{CCU} \\ \hline \frac{\Xi \vdash \iota \gg \epsilon \quad \epsilon' = \text{ctrl}(\gamma(q), \epsilon)}{\Xi \vdash \text{CU } p \iota \gg \epsilon'} \end{array} \quad \begin{array}{c} \text{CNEW} \\ \hline \frac{\Xi' = \Xi[\forall q \in \bar{q}. q \mapsto |\Xi| + \text{ind}(\bar{q}, q)]}{(n, \Xi, \text{new}(\bar{q})) \gg (n + |\bar{q}|, \Xi', \{\})} \end{array}$$

We show selected rules above; more are in Section C. Rules CRy and CCU are the instruction-level translation rules, which translate a PQASM instruction to a SQIR unitary operation. $\text{Ry}^r q$ has a directly corresponding gate in SQIR.

In the `CU` translation, the rule assumes that ι 's translation does not affect the Ξ position map. This requirement is assured for well-typed programs per rule `CU` in Figure 7. `ctrl` generates the controlled version of an arbitrary SQIR program using standard decompositions [39, Chapter 4.3].

Rule `CNEW` is one of the program-level rules, translating a qubit creation operation in PQASM. In SQIR, there is no qubit creation, in the sense that every qubit is assumed to exist in the first place. The translation essentially translates the operation to a `SKIP` operation in SQIR and increments the qubit heap size in the generated SQIR program.

Below is the translation correctness theorem. The proof utilizes the SQIR nondeterministic semantics, where a qubit measurement produces two possible outcomes with different probabilities associated with them, i.e., this nondeterministic semantics is essentially SQIR's way of describing a Markov-chain procedure. To formally state the correctness property, we relate PQASM superposition states Φ to SQIR states, as $\llbracket \Phi \rrbracket^{n'}$, which are vectors of $2^{n'}$ complex numbers. We can utilize Ξ to relate qubits in PQASM with qubit positions in SQIR.

Theorem 3. [Translation Correctness] Suppose $\Sigma; \Omega \vdash e \triangleright \Omega'$ and $(n, \Xi, e) \gg (n', \Xi', \chi)$. Then for $\Omega \vdash \Phi$ and $(\Phi, e) \xrightarrow{r} (\Phi', e')$, we have $(\llbracket \Phi \rrbracket^{n'}, \chi) \xrightarrow{r} (\llbracket \Phi' \rrbracket^{n'}, \chi')$ and $(n', \Xi', e') \gg (n'', \Xi'', \chi')$.

Proof. The proof is by induction on the PQASM program e . Most of the proof simply shows the correspondence of operations in e to their translated-to gates ϵ in SQIR, except for `new` and measurement operations, which update the Ξ map.

5 Evaluation: Applicativity via Case Studies

Here, an experimental evaluation of QSV across many programs is conducted to assess how QSV can be used to effectively build and validate useful quantum state preparation programs with different patterns. The efficiency and scalability comparison with other frameworks are in Section 6.

Implementation. We implement QSV in Rocq and utilize QuickChick to create a quantum program validation framework. We also provide a PQASM circuit compiler that translates PQASM programs to OpenQASM via SQIR.

Experimental Setup. We perform our evaluation on an Ubuntu computer, which has 8-core 13-gen i9 Intel processors and 16 GiB DDR5 memory.

We present several case studies here to demonstrate the construction and validation of state preparation programs. We classify *two different program patterns* below and examine their validation strategies. We list the qubit and gate counts for these programs in Figure 10. The data are collected by compiling our programs to SQIR using the elementary gateset $\{X, H, CX, Rz\}$. To describe the programs, we define the following repeat operator for repeating a process n times. The function P takes a natural number and outputs a quantum program.

$$Re(P, n) \triangleq \text{if } (n = 0) \{ \} \text{ else } Re(P, n - 1) ; P(n - 1)$$

State Preparation Program	8B Gate #	8B Qubit #	60B Gate #	60B Qubit #
n basis-ket	766	9	5,732	61
Modular Exponentiation	277K	27	3.3M	183
Amplitude Amplification	65	9	481	61
Hamming Weight	9,088	16	170K	120
Distinct Element	16,036	49	120K	361

Fig. 10: Program statistics; a single register with 8 and 60 Qubits (8B/60B); Distinct elements have 5 distinct elements (keys). ‘K’: thousand, ‘M’: million.

Quantum Loop Programs. We first examine the class of programs only involving quantum unitary gates without measurement. Such programs typically contain quantum loops, a repetition of subroutines formed via unitary gates. These programs usually act as a large part of some quantum algorithms. For example, the modular exponentiation state preparation program is the major part of Shor’s algorithm, while the amplitude amplification state preparation program is the major part of an upgraded amplitude estimation algorithm [50]. **Modular Exponentiation State Preparation.** In Shor’s algorithm [47], we prepare the the superposition state of modular exponentiation based on two natural numbers c and n with $\text{gcd}(c, n) = 1$, as $\varphi_3 = \frac{1}{\sqrt{2^m}} \sum_j^{2^m} |j\rangle_m |c^j \% n\rangle_m$.

$$\begin{aligned} Q(\overline{q_1}, \overline{q_2})(k) &\triangleq \text{CU}(\overline{q_1}[k]) (c^{2^k} * \overline{q_2}) \% n \\ P(m) &\triangleq \text{new}(\overline{q_1}) ; \text{new}(\overline{q_2}) ; \text{H}(\overline{q_1}) ; \text{Re}(Q(\overline{q_1}, \overline{q_2}), m) \end{aligned}$$

The program to prepare the modular exponentiation state is listed above, with the circuit diagram in Figure 11. The program starts with two new length m qubit arrays $\overline{q_1}$ and $\overline{q_2}$, and turns $\overline{q_1}$ to a uniform superposition by m H gates. We then repeat m times a controlled modular multiplication ($\text{CU}(\overline{q_1}[k]) (c^{2^k} * \overline{q_2}) \% n$) application, controlling on the qubit $\overline{q_1}[k]$ with application to $\overline{q_2}$.

As in Section 4.1, to conduct the the program correctness validation, we cut off the first three operations (new and H operations) in $P(m)$, producing a program piece $\text{Re}(Q(\overline{q_1}, \overline{q_2}), m)$, where $Q(\overline{q_1}, \overline{q_2})$ is a function taking in a number k and outputting a program $\text{CU}(\overline{q_1}[k]) (c^{2^k} * \overline{q_2}) \% n$. The correctness specification is also transformed without the superposition state description below.

$$\forall j \in [0, 2^m). |j\rangle_m |0\rangle_m \rightarrow |j\rangle_m |c^j \% n\rangle_m$$

Validating the loop program $\text{Re}(Q(\overline{q_1}, \overline{q_2}), m)$ essentially executes Q m times. In executing the k -th loop step, we have the following loop invariant.

$$|j\rangle_k |c^j \% n\rangle_m \rightarrow |j\rangle_{k+1} |c^j \% n\rangle_m$$

In the pre-state, $|j\rangle_k$ is a length k bitstring while the post-state has $|j\rangle_{k+1}$ being length $k+1$. To understand the behavior, notice that we have the most significant bit on the right. A $k+1$ length bitstring $|j\rangle_{k+1}$ can be expressed as a composition over a length k bitstring as $|j\rangle_k |0\rangle_1$ or $|j\rangle_k |1\rangle_1$, with the most

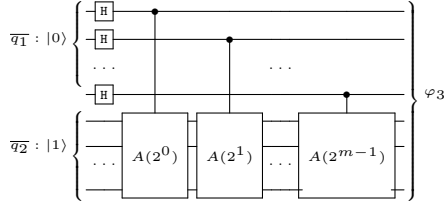


Fig. 11: Modular Exponentiation Circuits; $A(v) = (c^v * \bar{q}_2) \% n$.

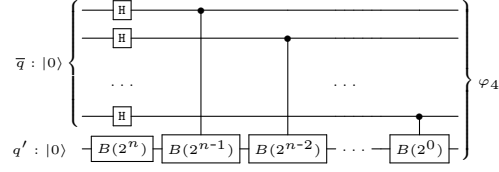


Fig. 12: Amplitude amplification state preparation; $B(v) = \text{Ry}(\frac{r}{v})$.

significant bit being 0 or 1. For the former case, applying the controlled modular multiplication results in $|j\rangle_k |0\rangle_1 |c^j \% n\rangle_m$, i.e., the \bar{q}_2 part of the bitstring remains the same. For the latter case ($|j\rangle_k |1\rangle_1$), the controlled modular multiplication results in the state $|j\rangle_k |1\rangle_1 |(c^{2^k} * c^j \% n) \% n\rangle_m = |j\rangle_k |1\rangle_1 |c^{j+2^k} \% n\rangle_m$. Both cases can be rewritten to the post-state in the loop invariant above.

To validate the program piece $Re(Q(\bar{q}_1, \bar{q}_2), m)$ against the above specification, we are given a length $2m$ bitstring with \bar{q}_1 and \bar{q}_2 both being length m , and view \bar{q}_1 as a length m array of random variables, and prepare a initial state $|\bar{q}_1[0], \dots, \bar{q}_1[m-1]\rangle_m |0\rangle_m$, with random generation of length m binary bitstrings, as test instances, for the variables $\bar{q}_1[0], \dots, \bar{q}_1[m-1]$. We then use the mechanism in Section 4.1 to validate the program piece. As we mentioned in Section 1, after we test enough samples of different input basis-ket states by picking different values for random variables, we have a high assurance that the modular exponentiation state preparation program correctly prepares a superposition state.

Note that the program is a deterministic quantum circuit program, so the probability of preparing the superposition state is 100%.

Amplitude Amplification State Preparation Through Ry Gates. In the amplitude amplification algorithm, one needs to prepare a special superposition state [50], as $\varphi_4 = \frac{1}{\sqrt{2^n}} \sum_{j=1}^{2^n} |j\rangle_n |\Delta(\frac{(2j+1)r}{2^n})\rangle$, circuit in Figure 12. Then, the amplitude amplification algorithm utilizes the last qubits ($|\Delta(\frac{(2j+1)r}{2^n})\rangle$) to amplify the amplitudes of the basis-kets having a particular property with respect to some j . The r value is the upper limit of the possible amplitude value, i.e., we want to carefully select r to ensure $\frac{(2j+1)r}{2^n} \in [0, \frac{\pi}{2})$.

$$\begin{aligned} Q(\bar{q}, q')(j) &\triangleq \text{CU}(\bar{q}[j]) \text{Ry}^{\frac{r}{2^n-j}} q' \\ P(n) &\triangleq \text{new}(\bar{q}); \text{new}(q'); \text{H}(\bar{q}); \text{Ry}^{\frac{r}{2^n}} q'; Re(Q(\bar{q}, q'), n) \end{aligned}$$

We implement the program P in PQASM with the input of a qubit array \bar{q} and a single qubit q' . We then apply H gates on \bar{q} and a Y-axis rotation on q' . Eventually, we apply a series of controlled Y-axis rotation operations — controlling on the $\bar{q}[j]$ qubit ($j \in [0, n)$) and applying Ry on q' ; each single controlled Y axis rotation is handled by the Q process.

Since there is no measurement, the success rate of preparing the amplitude amplification state is theoretically 100%. We mainly test the correctness here.

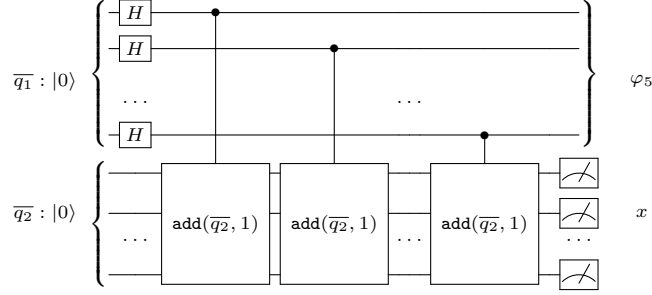


Fig. 13: One-step Hamming weight state preparation (repeat-until-success).

$$\text{Ry}^{\frac{\pi}{2^r}} q' ; \text{Re}(Q(\bar{q}, q'), n) \quad \forall j \in [0, 2^n) \cdot |j\rangle_n |0\rangle_1 \rightarrow |j\rangle_n |\Delta(\frac{(2j+1)r}{2^n})\rangle$$

In doing so, we can adapt the same strategy in the modular exponentiation state preparation, by cutting off $\text{new}(\bar{q}) ; \text{new}(q') ; \text{H}(\bar{q})$, so we should mainly focus on validating the portion shown above on the left. The correctness specification is described above on the right. In validating this portion, we notice that the qubit array \bar{q} is in Had type, and we generate random variables, with binary values 0 or 1, for every qubit in the array. Through the validation procedure in validating the modular exponentiation program above, we can assure that the result of the program produces the superposition state φ_4 .

Repeat-until-success Programs. We then examine the class of repeat-until-success programs, using the strategy in Section 4.1. We show the Hamming weight and the distinct element state preparation program validation below.

Hamming Weights State Preparation. Some algorithms [19] require a k -th Hamming weight superposition state preparation, i.e., we prepare a state $\varphi_5 = \frac{1}{\sqrt{N}} \sum_j^N |c_j\rangle_n$, with the number of 1's bit in c_j is k . Assuming that φ_5 is a length n qubit state, φ_5 has N different basis-kets, with $N = \binom{n}{k}$.

$$Q(\bar{q}_1, \bar{q}_2)(j) \triangleq \text{CU}(\bar{q}_1[j] \text{ add}(\bar{q}_2, 1))$$

$$P(n, k) \triangleq \text{new}(\bar{q}_1) ; \text{new}(\bar{q}_2) ; \text{H}(\bar{q}_1) ; \text{Re}(Q(\bar{q}_1, \bar{q}_2), n) ; \text{let } x = \mathcal{M}(\bar{q}_2) \text{ in if } (x=k) \{ \} \text{ else } P(n, k)$$

The above is a repeat-until-success program of the Hamming weight program, with the circuit in Figure 13 showing a single quantum step in $P(n, k)$. The program starts with two new length n qubit arrays \bar{q}_1 and \bar{q}_2 , and turns \bar{q}_1 to a uniform superposition by applying n H gates. We then repeat n times of a controlled addition ($\text{CU}(\bar{q}_1[j] \text{ add}(\bar{q}_2, 1))$) applications. The controlled additions count the number of 1's bits in \bar{q}_1 and store the result in \bar{q}_2 . If the measurement on \bar{q}_2 results in k (assigning to x), it means that the φ_5 state of the qubit array \bar{q}_1 is a superposition of basis-ket states with the vector having k bits of 1. Otherwise, we repeat the process P with two new qubit arrays \bar{q}_1 and \bar{q}_2 until

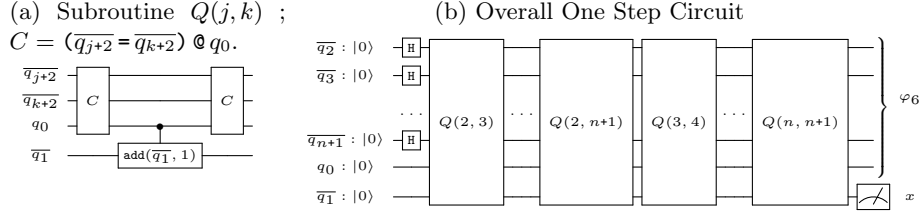


Fig. 14: One step distinct element state preparation.

the measurement result k appears. Note that $Q(\bar{q}_1, \bar{q}_2)$ in Re is a function taking in a natural number argument j and then performing a controlled addition.

$$\begin{aligned}
 & Re(Q(\bar{q}_1, \bar{q}_2), n) ; \text{let } x = \mathcal{M}(\bar{q}_2) \text{ in if } (x = k) \{ \} \text{ else } \{ \} \\
 & \forall j \in [0, 2^n). |j\rangle_n |0\rangle_n \rightarrow |j\rangle_n \wedge \text{sum}(\mathbf{n2b}(j)) = k
 \end{aligned}$$

To validate the correctness of the Hamming weight program, we shrink the program by removing the `new` and `H` operations. The program piece and the transformed correctness specification are listed above. We then utilize the procedure in Section 4.1 to perform the validation. Here, we assume that the `Had` typed qubits \bar{q}_1 are already prepared, and we randomly generate a length n bit-string for the random variables $\bar{q}_1[0], \dots, \bar{q}_1[n-1]$. Each random variable, possibly being 0 or 1, represents the basis-bit of a single qubit superposition. We set up the PBT to randomly sample values for the random variables and exclusively test the correctness of the transition behavior of basis-ket states. The key correctness property ($\text{sum}(\mathbf{n2b}(j)) = k$) for the Hamming weight state is that each output basis-ket of \bar{q}_1 should have exactly k bits of 1.

The program efficiency can be easily assessed by counting the number of basis kets in a superposition quantum state. Notice that every superposition state prepared by a simple Hadamard operation produces a uniform superposition, meaning that the likelihood of measuring out any basis-ket vector is equally likely. Thus, we only need to compare the ratio between the number of basis-kets after the Hadamard operations are applied and the basis-ket number in \bar{q}_1 after the measurement is applied. The former contains 2^n different basis-kets for n Hadamard operations, and the latter has $\binom{n}{k}$ basis-kets in a k -th Hamming weight state. So, the success rate of a single try in the program is $\binom{n}{k} / 2^n$.

Distinct Element State Preparation. Another special superposition state is the one in the element distinctness algorithm. Here, we assume that we are given a graph with n different vertices, and the algorithm begins with a superposition of different combinations of vertices, as shown below.

$$\varphi_6 = \frac{1}{\sqrt{n!}} \sum_j \sigma_j (|x_1\rangle |x_2\rangle \dots |x_n\rangle)$$

Here, x_1, x_2, \dots, x_n are different vertex keys in the graph, σ_j is a permutation of the key list $|x_1\rangle |x_2\rangle \dots |x_n\rangle$. There are $n!$ different kinds of permutations, so the uniform amplitude for each basis-ket is $\frac{1}{\sqrt{n!}}$. Such a permutation state means we are preparing a superposition of all permutations of the different vertex keys. Such a superposition state is widely used in many algorithms, such as the quantum fingerprinting algorithm [13].

```

Q(k)(j)  $\triangleq$  ( $\overline{q_{j+2}} = \overline{q_{k+2}}$ ) @  $q_0$  ; CU  $q_0$  ( $\overline{q_1} + 1$ ) ; ( $\overline{q_{j+2}} = \overline{q_{k+2}}$ ) @  $q_0$ 
R(j)(n)  $\triangleq$  Re(Q(j), n)
H(j)  $\triangleq$  H( $\overline{q_{j+2}}$ )
T(j)  $\triangleq$  new( $\overline{q_{j+1}}$ )
P(n)  $\triangleq$  new( $q_0$ ) ; Re(T, n+1) ; Re(H, n) ; Re(R(n-1), n) ; let  $x = \mathcal{M}(\overline{q_1})$  in if ( $x=0$ ) {} else P(n)

```

For simplicity, we only implement the above program to prepare a superposition state of distinct elements, i.e., each basis-ket in the superposition state stores n distinct elements (vertex key), each key having a qubit size m . Note that if $n = 2^m$, i.e., we have 2^m different vertices having keys $u \in [0, 2^m)$, then the superposition state represents a superposition of all the permutations. We show a repeat-until-success program for preparing such a state above, with the circuit in Figure 14 showing a single quantum step in $P(n)$. We first initialize a single qubit q_0 , and use $T(j)$ to initialize $n + 1$ different qubit arrays, $\overline{q_{j+1}}$, with $j \in [0, n + 1)$, and we assume that $\overline{q_{j+1}}$ is an m length qubit array. We then apply H gates to all qubit arrays $\overline{q_{j+2}}$ ($j \in [0, n)$). q_0 and $\overline{q_1}$ are ancillary qubits.

Essentially, we can view $\overline{q_{j+2}}$ ($j \in [0, n)$) as an n -length array of qubit arrays. The program applies $O(n^2)$ times of Q processes, each of which applies an equivalent check on two elements in the n -length array, i.e., we compare the basis-ket data in q_{j+2} and q_{k+2} ($j, k \in [0, n)$) to see if their content are equal, and store the boolean result in q_0 bit. Then, we also add the result to $\overline{q_1}$ and apply the comparison circuit again to clean up the ancillary qubit q_0 , meaning that we restore q_0 's state to $|0\rangle$. This procedure describes the circuit in Figure 14a.

After we apply the Q function to any two different elements in the n -length array, we observe that q_0 is back to the $|0\rangle$ state, and $\overline{q_1}$ stores the number of same basis-kets between any two distinct elements in the n -length array. We then measure $\overline{q_1}$ and see if the result is 0. If so, a permutation superposition state is prepared because it means that in all the basis-kets in the prepared superposition, there are no two-qubit array elements $\overline{q_k}$ and $\overline{q_l}$ that have equal key. If not, we repeat the process, and the repeat-until-success program guarantees the creation of the permutation superposition state.

We use the procedure in Section 4.1 to validate the correctness. We create the validating program by removing the new and H operations from the original program. The program piece and the transformed specification are listed below.

$$\begin{aligned}
& \text{Re}(R(n-1), n) ; \text{let } x = \mathcal{M}(\overline{q_1}) \text{ in if } (x=0) \{ \} \text{ else } \{ \} \\
& x=0 \Rightarrow \forall j, j' \in [0, 2^{n*m}). |0\rangle_1 |0\rangle_n |j\rangle_{n*m} \rightarrow |0\rangle_1 |j'\rangle_{n*m} \wedge \text{dis}(j', m)
\end{aligned}$$

Here, j and j' represent the values for two qubit arrays, i.e., j represents the bitstring value for composing basis-ket values of all elements in the qubit array

Program	QSV QCT 8B	QSV QCT 60B	Qiskit Sim 8B	Qiskit Sim 60B	DDSim Sim 60B
n basis-ket	< 1.5	2.4	< 1.5	No	No
Modular Exp.	< 1.5	19.7	No	No	No
Amplitude Amp.	< 1.5	2.1	< 1.5	No	No
Hamming Weight	< 1.5	24.9	< 1.5	No	No
Distinct Element	< 5	336	No	No	No

Fig. 15: Evaluation on different state preparation programs for 8/60 qubit single registers (8B/60B). "QCT" : time (in seconds) for QuickChick to run 10,000 tests. "Sim": time (in seconds) or if Qiskit/DDSim can execute a single test.

$\overline{q_{l+2}}$ ($l \in [0, n)$). The qubit array $\overline{q_{j+2}}$ has $n*m$ qubits, and we slice the basis-vector for the whole qubit array into n different small segments for the qubit ranges $[l*m, l*(m+1)-1)$, each basis-vector segment representing a vertex key. Since we apply Hadamard operations to all of them, it creates a uniform superposition state containing 2^{n*m} different basis-vector states. In the post-state of the specification, the q_0 qubit is still $|0\rangle$. For the qubit arrays $\overline{q_2}, \dots, \overline{q_{m+2}}$, if the measurement result is $x = 0$, we result in a superposition state of distinct elements, i.e., any two elements (each element l is a segment of $[l*m, l*(m+1)-1)$) in the qubit array $\overline{q_{j+2}}$ have distinct basis-vectors. We use the predicate $\text{dis}(j', m)$ to indicate that all length m segments in the bitstring $|j\rangle$ are pairwise distinct. Via our PBT framework, we have high assurance that the distinct element state preparation program correctly prepares the superposition state.

The program's efficiency in preparing the superposition state can be easily assessed by counting the number of basis-ket states in the superposition. Notice that every superposition state prepared by a simple Hadamard operation produces a uniform superposition, meaning that the likelihood of measuring out any basis state vectors is equally likely. Thus, we only need to compare the ratio between the number of basis-kets right after the Hadamard operations are applied and the basis-ket number in $\overline{q_{j+2}}$. Here, we count the case for $n = 2^m$ where a permutation superposition state is prepared. For $j \in [0, n)$ with $n = 2^m$, after the measurement is applied. The former contains 2^{n*m} different basis-kets for $n*m$ Hadamard operations, and the latter has $n!$ basis-kets in a k -th permuted superposition state. So, the success rate of a single try in the program is $\frac{n!}{2^{n*m}}$.

6 Discussion: Efficiency, Scalability, and Utility

We compare QSV's efficiency and scalability with the state-of-the-art platforms. We show that QSV can effectively validate program properties, providing confidence in program correctness. We also show that QSV *scales* to validate and realize state preparation programs regardless of the size (in terms of qubit number required). We thus justify the QSV's utility in successfully capturing bugs.

Efficiency. We discuss the program development procedure in QSV, compared to other systems such as Qiskit. Discussing the efficiency of a validation frame-

work needs to be put in the context of human efforts for program development, as users mainly care about how to effectively use QSV to develop programs.

The general procedure for developing state preparation programs in QSV is the traditional test-driven program development. We first present the program correctness properties in the superposition state format for different programs, such as the one in Sections 1 and 5. We then start implementing the program using a possible program pattern and see if we can write the correct program based on it, where the PQASM high-level abstraction helps us write programs. For example, in dealing with all the programs in Figure 10, we first try to see if we can write all these programs via the quantum loop program pattern, and rewrite the correctness properties based on the strategy presented in Section 5.

We then run the QSV validator to validate the implemented programs against the properties. After several rounds of corrections, one can typically judge whether the program is implementable. For example, using our validator, we found that implementing the Hamming weight and distinct element programs based on the quantum loop program pattern might be hard. We then switch to other program patterns to implement these programs; e.g., we use the repeat-until-success program pattern to implement the two programs by rewriting their correctness properties to those in Section 5 and successfully find a solution. Our validator can effectively validate a program using our PBT framework, which generates 10,000 test cases each time. As shown in Figure 15, running 10,000 randomly generated test cases for all our example programs takes less than 5 seconds for small-size programs (8 qubits) and less than 5.5 minutes for large-size programs (60 qubits). This indicates that a program developer can quickly correct minor bugs when developing their programs.

On the other hand, developing state preparation programs in the state-of-the-art system might be painful, e.g., it is unlikely one can perform test-driven development to implement the programs in Figure 10, mainly because of a lack of proper validation facilities. As we can see in Figure 15, Qiskit might not execute a single test for some small-size (8 qubit) programs, such as distinct-element programs. The modular exponentiation program is executed for some small number settings, but is not executable in general because the Qiskit simulator applies special optimizations to components of Shor’s algorithm. Executing a large program (60 qubits) is completely impossible; either the program is too large for IBM’s Aer simulator to run at all, and the simulator errors out, or the circuit construction may take hours and still not be done. This indicates the difficulty of developing large-scale programs by conducting small-scale testing in Qiskit, not to mention the need to validate large datasets and coverage. Another key issue is that the high-level abstraction support in the state-of-the-art systems is not well provided. In Qiskit, we can only find quantum addition operations; the other arithmetic and comparison operations are missing. In fact, we implement these operations in Qiskit based on our implementation in QSV.

Scalability. To evaluate the QSV’s scalability, we not only compare its execution at small and large sizes with Qiskit but also with another state-of-the-art quantum simulator, DDSim. Here, we attempted to recreate (or find existing

implementations of) the aforementioned programs on DDSim and Qiskit. We also performed PBT on our PQASM implementations on systems of various sizes and verified the rigidity of our tests by mutating either the properties or the states and verifying that the tests failed.

As in Figure 15, we have fully validated the five examples in these papers via our PBT framework. As far as we know, these constitute the first validated-correct implementations of the n basis-ket, Hamming weight, and distinct elements programs. All other operations in the figure were validated with QuickChick. To ensure these tests were effective, besides our program development procedures above, we also confirmed they could find hand-injected bugs; e.g., we changed the rotation angles in the Ry gate in the amplitude amplification state preparation and performed some mutation testing (e.g. replacing some non-skip terms with `{}` (skip) operations) and confirmed that our PBT could catch the inserted bugs. The tables in Figure 15 give the running times for our validator to validate programs—the times include the cost of compiling the Rocq code and running it with 10,000 randomly generated inputs via QuickChick. We validated these programs on small (8-qubit) and large (60-qubit) inputs (the numbers relevant to the reported qubit and gate sizes in Figure 10), with all validation completed within 2.5 minutes (most within seconds). For comparison, we translated our programs to SQIR, converted the SQIR programs to OpenQASM 2.0 [22], and then attempted to simulate the resulting circuits on a *single test input* using DDSim [14], a state-of-the-art quantum simulator, and listed the result in the fifth column. Unsurprisingly, the simulation of the 60-bit versions did not complete when running overnight. The third and fourth columns in Figure 15 show the results for executing a *single program run* in Qiskit, and Qiskit executes a few small-size programs (Section 6) and none of the large-size programs. The experiment provided strong assurance of QSV’s scalability.

There is a difference in the program execution between DDSim and QSV. The latter abstracts arithmetic operations and assumes they can be handled by the previous VQO [32] framework, whereas DDSim executes the entire circuits generated from a QSV program. To compare the effects, we list the QuickChick testing time (running 10,000 tests) for the operations used in our state preparation programs in Figure 16; these running time data were provided in

Operation	QCT
Addition	2
Comparison	5
Modular Multiplication	794

Fig. 16: Arith OP QC time (60B).

VQO. The addition and comparison circuits do not greatly affect the execution of our PQASM programs. Validating modular multiplication circuits might be costly, as our 60-bit modular exponentiation involves 60 modular multiplication operations. However, a typical validation scheme might only validate the correctness of a costly subcomponent once and then use its semantic properties to validate other programs that use it. More importantly, the purpose of the experiment of DDSim/Qiskit executions is to show the state-of-the-art impossibility of

executing quantum programs on a classical computer, while our QSV framework can validate quantum programs.

Utility. One of the utilities of a program validation framework is to find bugs or faults in the existing algorithms. During the development of the above programs, we identified several issues in two original algorithms [13,5] that utilize these special superposition states. Both algorithms require preparing a superposition state of distinct elements (or of permutations of distinct elements), but they do not specify how to effectively prepare such a state. To the best of our knowledge, the state preparation program in Section 5 is the first program implementation of the state via the repeat-until-success scheme. As our probability analysis shows, the likelihood of preparing such a state is not very high. This fact might indicate that the quantum algorithms’ advantage arguments over classical algorithms in these works are not solid, given the unclear preparation of the initial states. Without our implementations of these state preparation programs, it is impossible to detect these subtle potential faults in these algorithms.

Indeed, in the algorithm [19] that uses the initial Hamming-weight superposition state, the authors recognized the low probability of preparing the initial state via the repeat-until-success scheme and proposed using a specialized gate instead of Hadamard gates to start their repeat-until-success state preparation program. The special gates created a simple superposition state with a different probability distribution, unlike the uniform distribution produced by Hadamard gates. The analysis of these specialized superposition gates with different probability distributions will be included in our future work.

Another utility of using QSV is to judge the implemented programs’ correctness and find a more optimized implementation. Other frameworks, such as OpenQASM, do not have property-based testing features.

7 Related Work

This section gives related work beyond the discussion in Section 4.

Quantum Circuit Languages. Prior research has developed circuit-level compilers to compile quantum circuit languages to quantum computers, such as Qiskit [4], t|ket) [15], Staq [8], PyZX [30], Nam *et al.* [38], quilc [45], Cirq [25], Scaffold [29], and Project Q [49]. In addition, many quantum programming languages have been developed in recent years. Many of these languages (e.g. Quil [45], OpenQASM [22,21], SQIR [28]) describe low-level circuit programs. Higher-level languages may provide library functions for performing common oracle operations (e.g., Q# [37], Scaffold [2,34]) or support compiling from classical programs to quantum circuits (e.g., Quipper [26]), but still leave some important details (like deallocating extra intermediate qubits) to the programmer. There has been some work on type systems to enforce that deallocation happens correctly (e.g., Silq [12]) and on automated insertion of deallocation circuits (e.g., Quipper [26], Unqomp [42]), but while these approaches provide useful automation, they may also lead to inefficiencies in compiled circuits.

Quantum Software Testing and Validation. There have been many approaches developed for validating quantum programs [40,55,53,23,35,52] including the use differential [52] and metamorphic testing [41], and mutation testing [23] and fuzzing [55]. Some key challenges exist for testing quantum programs. First, their input space explodes due to superposition. Second, their results are probabilistic (meaning we need to use statistical measures and/or other approaches to evaluate results). Last, the expected result may be difficult or even impossible to determine. To date, testing approaches have focused on validating small circuit subroutines (i.e., with limited input qubit size) rather than comprehensive quantum programs, and they are all limited to testing in Qiskit, which might not capture all machine limitations.

Methodologies Possibly Used for Validating Quantum Programs. SymQV [10] proposed a method of encoding quantum states and gates as SMT-solvable predicates to perform automated verification. Chen *et al.* [16] and Abdulla *et al.* [1] used tree automata to symbolize quantum gates, instead of quantum states, and utilized tree automata to construct a tree structure for easing automated verification. These works can handle some large programs, but these programs have simple program structures, such as QFT. Mei *et al.* [36] performed quantum stabilizer simulation based on the Gottesman–Knill theorem, which is a small subset of quantum programs and mainly used for error correction programs. Quasimodo [48] is another symbolic execution based on a BDD-like structure to symbolize gates rather than states; their results are similar to the tree automata works [1,16]. QAFNY [33,17] transformed quantum program verification to Dafny for automated verification. These works tried to transform states and gates to perform automated verification, different from QSV, which tries to perform program testing and validation. The methodologies are also different from QSV where they try to symbolize quantum gates and states, while QSV only inserts special treatments in the standard quantum state representations. As a result, QSV can deal with large programs with comprehensive program structures.

Verified Quantum Compilers. Recent work has looked at verified optimization of quantum circuits (e.g., VOQC [28], CertiQ [46]), but the problem of verified *compilation* from high-level languages to quantum circuits has received less attention. The only examples we know of verified compilers for quantum circuits are ReVerC [9], ReQWIRE [44], and Feynman [7] [6]. ReVerC and ReQWIRE support verified translation from a low-level Boolean expression language to circuits consisting of X, CNOT, and CCNOT gates. Feynman verifies the correctness of compiled circuits relative to an input circuit or a path-integral specification of a circuit, while QSV validates whether programs have specified properties before they are compiled to the circuit level. It’s feasible that a programmer can use QSV to validate the program and then use Feynman to verify the compiled circuit relative to a circuit or path integral specification of the program. VQO [32] is a certified compilation framework for verifying and compiling quantum arithmetic operations. QSV utilizes VOQC [28] and VQO [32] to compile PQASM programs to quantum circuits.

8 Conclusion and Limitations

We present QSV, a framework for expressing and automatically validating quantum state preparation programs. The core of QSV is a language PQASM, which can express a restricted class of quantum programs that are efficiently testable for certain properties and are useful for implementing state preparation programs. We have verified the translator from PQASM to SQIR and have validated (or randomly tested) many programs written in PQASM. We have used PQASM to implement state preparation programs useful in quantum computation, such as the ones in Figure 10. We hope this work will be the basis for building a quantum validation framework for validating quantum programs on classical computers.

QSV is capable of validating properties of many quantum programs. As mentioned in Section 1, QSV targets validating state preparation programs. For many quantum programs, QSV is able to validate the most significant part of the program. For example, the validated modular multiplication program in Figure 11 is essentially 90% of Shor’s algorithm, except for the final inverse QFT gate and measurement.

Our type system specifically locates Hadamard operations, but there are no actual restrictions on Hadamard operations, as users can easily define similar behaviors via our Ry and oracle operations. Via our type system, we identify the beginning Hadamard operations as a general quantum algorithm component to generate superposition sources so that QSV can locate the places to create random inputs for validating programs. We recognize the superposition state generation in many quantum algorithms as the major bottleneck for testing quantum programs; therefore, we utilize types to identify them, with special treatment to transform the superposition states to a simple and testable format.

9 Data-Availability Statement

The Rocq proofs and the experiment in the paper are available on Zenodo: <https://doi.org/10.5281/zenodo.15073729> [31]. The Zenodo artifact can be run in the experimental setting described in its README. There is also a GitHub repository at <https://github.com/qafny/pqasm>.

References

1. Abdulla, P.A., Chen, Y.G., Chen, Y.F., Holík, L., Lengál, O., Lin, J.A., Lo, F.Y., Tsai, W.L.: Verifying quantum circuits with level-synchronized tree automata (technical report) (2024), <https://arxiv.org/abs/2410.18540>
2. Abhari, A., Faruque, A., Dousti, M.J., Svec, L., Catu, O., Chakrabati, A., Chiang, C.F., Vanderwilt, S., Black, J., Chong, F., Martonosi, M., Suchara, M., Brown, K., Pedram, M., Brun, T.: Scaffold: Quantum Programming Language. Tech. rep., Princeton University (2012)
3. Alagic, G., Moore, C., Russell, A.: Quantum algorithms for simon’s problem over general groups (2007), <https://arxiv.org/abs/quant-ph/0603251>

4. Aleksandrowicz, G., Alexander, T., Barkoutsos, P., Bello, L., Ben-Haim, Y., Bucher, D., Cabrera-Hernández, F.J., Carballo-Franquis, J., Chen, A., Chen, C.F., Chow, J.M., Córcoles-Gonzales, A.D., Cross, A.J., Cross, A., Cruz-Benito, J., Culver, C., González, S.D.L.P., Torre, E.D.L., Ding, D., Dumitrescu, E., Duran, I., Eendebak, P., Everitt, M., Sertage, I.F., Frisch, A., Fuhrer, A., Gambetta, J., Gago, B.G., Gomez-Mosquera, J., Greenberg, D., Hamamura, I., Havlicek, V., Hellmers, J., Herok, L., Horii, H., Hu, S., Imamichi, T., Itoko, T., Javadi-Abhari, A., Kanazawa, N., Karazeev, A., Krsulich, K., Liu, P., Luh, Y., Maeng, Y., Marques, M., Martín-Fernández, F.J., McClure, D.T., McKay, D., Meesala, S., Mezzacapo, A., Moll, N., Rodríguez, D.M., Nannicini, G., Nation, P., Ollitrault, P., O’Riordan, L.J., Paik, H., Pérez, J., Phan, A., Pistoia, M., Prutyaynov, V., Reuter, M., Rice, J., Davila, A.R., Rudy, R.H.P., Ryu, M., Sathaye, N., Schnabel, C., Schoute, E., Setia, K., Shi, Y., Silva, A., Siraichi, Y., Sivarajah, S., Smolin, J.A., Soeken, M., Takahashi, H., Tavernelli, I., Taylor, C., Taylour, P., Trabing, K., Treinish, M., Turner, W., Vogt-Lee, D., Vuillot, C., Wildstrom, J.A., Wilson, J., Winston, E., Wood, C., Wood, S., Wörner, S., Akhalwaya, I.Y., Zoufal, C.: Qiskit: An open-source framework for quantum computing (2019). <https://doi.org/10.5281/zenodo.2562110>
5. Ambainis, A.: Quantum walk algorithm for element distinctness. In: 45th Annual IEEE Symposium on Foundations of Computer Science. pp. 22–31 (2004). <https://doi.org/10.1109/FOCS.2004.54>
6. Amy, M.: Formal Methods in Quantum Circuit Design. Ph.D. thesis, University of Waterloo (2019)
7. Amy, M.: Towards large-scale functional verification of universal quantum circuits. *Electronic Proceedings in Theoretical Computer Science* **287**, 1–21 (Jan 2019). <https://doi.org/10.4204/eptcs.287.1>, <http://dx.doi.org/10.4204/EPTCS.287.1>
8. Amy, M., Gheorghiu, V.: staq – a full-stack quantum processing toolkit **5**(3), 034016 (Jun 2020). <https://doi.org/10.1088/2058-9565/ab9359>, <https://github.com/softwareQinc/staq>
9. Amy, M., Roetteler, M., Svore, K.M.: Verified Compilation of Space-Efficient Reversible Circuits. In: Majumdar, R., Kunčák, V. (eds.) *Computer Aided Verification*. pp. 3–21. Springer International Publishing, Cham (2017)
10. Bauer-Marquart, F., Leue, S., Schilling, C.: symqv: Automated symbolic verification of quantum programs. In: *Formal Methods: 25th International Symposium, FM 2023, Lübeck, Germany, March 6–10, 2023, Proceedings*. p. 181–198. Springer-Verlag, Berlin, Heidelberg (2023). https://doi.org/10.1007/978-3-031-27481-7_12, https://doi.org/10.1007/978-3-031-27481-7_12
11. Beauregard, S.: Circuit for shor’s algorithm using $2n+3$ qubits. *Quantum Info. Comput.* **3**(2), 175–185 (Mar 2003)
12. Bichsel, B., Baader, M., Gehr, T., Vechev, M.: Silq: A High-Level Quantum Language with Safe Uncomputation and Intuitive Semantics. In: *Proceedings of the 41st ACM SIGPLAN Conference on Programming Language Design and Implementation*. p. 286–300. PLDI 2020, Association for Computing Machinery, New York, NY, USA (2020). <https://doi.org/10.1145/3385412.3386007>, <https://doi.org/10.1145/3385412.3386007>
13. Buhrman, H., Cleve, R., Watrous, J., de Wolf, R.: Quantum fingerprinting. *Physical Review Letters* **87**(16) (Sep 2001). <https://doi.org/10.1103/physrevlett.87.167902>, <http://dx.doi.org/10.1103/PhysRevLett.87.167902>
14. Burgholzer, L., Bauer, H., Wille, R.: Hybrid Schrödinger-Feynman Simulation of Quantum Circuits With Decision Diagrams . In: *2021 IEEE International Con-*

- ference on Quantum Computing and Engineering (QCE). pp. 199–206. IEEE Computer Society, Los Alamitos, CA, USA (Oct 2021). <https://doi.org/10.1109/QCE52317.2021.00037>, <https://doi.ieeecomputersociety.org/10.1109/QCE52317.2021.00037>
15. Cambridge Quantum Computing Ltd: pytket (2019), <https://cqcl.github.io/pytket/build/html/index.html>
 16. Chen, Y.F., Chung, K.M., Lengál, O., Lin, J.A., Tsai, W.L., Yen, D.D.: An automata-based framework for verification and bug hunting in quantum circuits. *Proc. ACM Program. Lang.* **7**(PLDI) (Jun 2023). <https://doi.org/10.1145/3591270>, <https://doi.org/10.1145/3591270>
 17. Cheng, F., Vangeepuram, S., Allard, H., Jafari, S.M.R., Potanin, A., Li, L.: Embedding quantum program verification into dafny. *Proc. ACM Program. Lang.* **9**(OOPSLA2) (Oct 2025). <https://doi.org/10.1145/3763157>, <https://doi.org/10.1145/3763157>
 18. Childs, A., Reichardt, B., Spalek, R., Zhang, S.: Every NAND formula of size N can be evaluated in time $N^{1/2+o(1)}$ on a Quantum Computer (03 2007)
 19. Childs, A.M., Farhi, E., Goldstone, J., Gutmann, S.: Finding cliques by quantum adiabatic evolution. *Quantum Info. Comput.* **2**(3), 181–191 (Apr 2002)
 20. Claessen, K., Hughes, J.: Quickcheck: A lightweight tool for random testing of haskell programs. In: *Proceedings of the Fifth ACM SIGPLAN International Conference on Functional Programming*. p. 268–279. ICFP '00, Association for Computing Machinery, New York, NY, USA (2000). <https://doi.org/10.1145/351240.351266>, <https://doi.org/10.1145/351240.351266>
 21. Cross, A., Javadi-Abhari, A., Alexander, T., De Beaudrap, N., Bishop, L.S., Heidel, S., Ryan, C.A., Sivarajah, P., Smolin, J., Gambetta, J.M., Johnson, B.R.: Openqasm 3: A broader and deeper quantum assembly language. *ACM Transactions on Quantum Computing* **3**(3) (sep 2022). <https://doi.org/10.1145/3505636>, <https://doi.org/10.1145/3505636>
 22. Cross, A.W., Bishop, L.S., Smolin, J.A., Gambetta, J.M.: Open quantum assembly language. arXiv e-prints (Jul 2017)
 23. Fortunato, D., Campos, J., Abreu, R.: Mutation testing of quantum programs written in qiskit. In: *Proceedings of the ACM/IEEE 44th International Conference on Software Engineering: Companion Proceedings*. p. 358–359. ICSE '22, Association for Computing Machinery, New York, NY, USA (2022). <https://doi.org/10.1145/3510454.3528649>, <https://doi.org/10.1145/3510454.3528649>
 24. Gill, S.S., Cetinkaya, O., Marrone, S., Claudino, D., Haunschild, D., Schlote, L., Wu, H., Ottaviani, C., Liu, X., Machupalli, S.P., Kaur, K., Arora, P., Liu, J., Farouk, A., Song, H.H., Uhlig, S., Ramamohanarao, K.: Quantum computing: Vision and challenges (2024), <https://arxiv.org/abs/2403.02240>
 25. Google Quantum AI: Cirq: An Open Source Framework for Programming Quantum Computers (2019), <https://quantumai.google/cirq>
 26. Green, A.S., Lumsdaine, P.L., Ross, N.J., Selinger, P., Valiron, B.: Quipper: A scalable quantum programming language. In: *Proceedings of the 34th ACM SIGPLAN Conference on Programming Language Design and Implementation*. p. 333–342. PLDI '13, Association for Computing Machinery, New York, NY, USA (2013). <https://doi.org/10.1145/2491956.2462177>, <https://doi-org.proxy-um.researchport.umd.edu/10.1145/2491956.2462177>
 27. Hietala, K., Rand, R., Hung, S.H., Li, L., Hicks, M.: Proving quantum programs correct. In: *Proceedings of the Conference on Interactive Theorem Proving (ITP)* (Jun 2021)

28. Hietala, K., Rand, R., Li, L., Hung, S.H., Wu, X., Hicks, M.: A verified optimizer for quantum circuits. *ACM Trans. Program. Lang. Syst.* **45**(3) (Sep 2023). <https://doi.org/10.1145/3604630>, <https://doi.org/10.1145/3604630>
29. Javadi-Abhari, A., Patil, S., Kudrow, D., Heckey, J., Lvov, A., Chong, F.T., Martonosi, M.: ScaffCC: Scalable Compilation and Analysis of Quantum Programs. *Parallel Computing* **45**, 2–17 (Jun 2015). <https://doi.org/10.1016/j.parco.2014.12.001>
30. Kissinger, A., van de Wetering, J.: PyZX: Large scale automated diagrammatic reasoning. *Electronic Proceedings in Theoretical Computer Science* **318**, 230–242 (04 2020). <https://doi.org/10.4204/EPTCS.318.14>
31. Li, L., Sharma, A., Tagba, Z.D., Frett, S., Potanin, A.: Code for Validating Quantum State Preparation (Feb 2026). <https://doi.org/10.5281/zenodo.15073729>
32. Li, L., Voichick, F., Hietala, K., Peng, Y., Wu, X., Hicks, M.: Verified compilation of quantum oracles. *Proc. ACM Program. Lang.* **6**(OOPSLA2) (Oct 2022). <https://doi.org/10.1145/3563309>, <https://doi.org/10.1145/3563309>
33. Li, L., Zhu, M., Cleaveland, R., Nicoletti, A., Lee, Y., Chang, L., Wu, X.: Qafny: A Quantum-Program Verifier. In: Aldrich, J., Salvaneschi, G. (eds.) *38th European Conference on Object-Oriented Programming (ECOOP 2024)*. *Leibniz International Proceedings in Informatics (LIPIcs)*, vol. 313, pp. 24:1–24:31. Schloss Dagstuhl – Leibniz-Zentrum für Informatik, Dagstuhl, Germany (2024). <https://doi.org/10.4230/LIPIcs.ECOOP.2024.24>, <https://drops.dagstuhl.de/entities/document/10.4230/LIPIcs.ECOOP.2024.24>
34. Litteken, A., Fan, Y.C., Singh, D., Martonosi, M., Chong, F.T.: An updated LLVM-based quantum research compiler with further OpenQASM support. *Quantum Science and Technology* **5**(3), 034013 (may 2020). <https://doi.org/10.1088/2058-9565/ab8c2c>, <https://doi.org/10.1088/2058-9565/ab8c2c>
35. Long, P., Zhao, J.: Testing multi-subroutine quantum programs: From unit testing to integration testing. *ACM Trans. Softw. Eng. Methodol.* (apr 2024). <https://doi.org/10.1145/3656339>, <https://doi.org/10.1145/3656339>, just Accepted
36. Mei, J., Bonsangue, M., Laarman, A.: Simulating quantum circuits by model counting. In: Gurfinkel, A., Ganesh, V. (eds.) *Computer Aided Verification*. pp. 555–578. Springer Nature Switzerland, Cham (2024)
37. Microsoft: The Q# Programming Language (2017), <https://docs.microsoft.com/>
38. Nam, Y., Ross, N.J., Su, Y., Childs, A.M., Maslov, D.: Automated optimization of large quantum circuits with continuous parameters. *npj Quantum Information* **4**(1), 23 (May 2018). <https://doi.org/10.1038/s41534-018-0072-4>, <https://doi.org/10.1038/s41534-018-0072-4>
39. Nielsen, M.A., Chuang, I.L.: *Quantum Computation and Quantum Information*. Cambridge University Press, USA, 10th anniversary edn. (2011)
40. Paltenghi, M., Pradel, M.: Bugs in quantum computing platforms: an empirical study. *Proceedings of the ACM on Programming Languages* **6**(OOPSLA1), 1–27 (Apr 2022). <https://doi.org/10.1145/3527330>, <http://dx.doi.org/10.1145/3527330>
41. Paltenghi, M., Pradel, M.: Morphq: Metamorphic testing of the qiskit quantum computing platform. In: *Proceedings of the 45th International Conference on Software Engineering*. p. 2413–2424. ICSE '23, IEEE Press (2023). <https://doi.org/10.1109/ICSE48619.2023.00202>, <https://doi.org/10.1109/ICSE48619.2023.00202>

42. Paradis, A., Bichsel, B., Steffen, S., Vechev, M.: Unqomp: Synthesizing uncomputation in quantum circuits. In: Proceedings of the 42nd ACM SIGPLAN International Conference on Programming Language Design and Implementation. p. 222?236. PLDI 2021, Association for Computing Machinery, New York, NY, USA (2021). <https://doi.org/10.1145/3453483.3454040>, <https://doi.org/10.1145/3453483.3454040>
43. Paraskevopoulou, Z., HriTcu, C., Dénès, M., Lampropoulos, L., Pierce, B.C.: Foundational property-based testing. In: Urban, C., Zhang, X. (eds.) Interactive Theorem Proving. pp. 325–343. Springer International Publishing, Cham (2015). https://doi.org/10.1007/978-3-319-22102-1_22
44. Rand, R., Paykin, J., Lee, D.H., Zdancewic, S.: Reqwire: Reasoning about reversible quantum circuits. In: QPL (2018)
45. Rigetti Computing: The @rigetti optimizing Quil compiler (2019), <https://github.com/rigetti/quilc>
46. Shi, Y., Li, X., Tao, R., Javadi-Abhari, A., Cross, A.W., Chong, F.T., Gu, R.: Contract-based verification of a realistic quantum compiler. arXiv e-prints (Aug 2019)
47. Shor, P.: Algorithms for quantum computation: discrete logarithms and factoring. In: Proceedings 35th Annual Symposium on Foundations of Computer Science. pp. 124–134 (1994). <https://doi.org/10.1109/SFCS.1994.365700>
48. Sistla, M., Chaudhuri, S., Reps, T.: Symbolic quantum simulation with quasisimodo. In: Computer Aided Verification: 35th International Conference, CAV 2023, Paris, France, July 17–22, 2023, Proceedings, Part III. p. 213–225. Springer-Verlag, Berlin, Heidelberg (2023). https://doi.org/10.1007/978-3-031-37709-9_11, https://doi.org/10.1007/978-3-031-37709-9_11
49. Steiger, D.S., Haner, T., Troyer, M.: ProjectQ: an open source software framework for quantum computing. *Quantum* **2**, 49 (Jan 2018). <https://doi.org/10.22331/q-2018-01-31-49>, <http://dx.doi.org/10.22331/q-2018-01-31-49>
50. Suzuki, Y., Uno, S., Raymond, R., Tanaka, T., Onodera, T., Yamamoto, N.: Amplitude Estimation Without Phase Estimation. *Quantum Information Processing* **19**(2) (Jan 2020). <https://doi.org/10.1007/s11128-019-2565-2>, <https://doi.org/10.1007/s11128-019-2565-2>
51. Swayne, M.: What Are The Remaining Challenges Of Quantum Computing? (2023), <https://thequantuminsider.com/2023/03/24/quantum-computing-challenges/>
52. Wang, J., Zhang, Q., Xu, G.H., Kim, M.: Qdiff: Differential testing of quantum software stacks. In: 2021 36th IEEE/ACM International Conference on Automated Software Engineering (ASE). pp. 692–704 (2021). <https://doi.org/10.1109/ASE51524.2021.9678792>
53. Wang, X., Arcaini, P., Yue, T., Ali, S.: Quito: a coverage-guided test generator for quantum programs. In: Proceedings of the 36th IEEE/ACM International Conference on Automated Software Engineering. p. 1237–1241. ASE '21, IEEE Press (2022). <https://doi.org/10.1109/ASE51524.2021.9678798>, <https://doi.org/10.1109/ASE51524.2021.9678798>
54. Wootters, W.K., Zurek, W.H.: The no-cloning theorem . <https://doi.org/10.1063/pt.grxx.gcmb>
55. Xia, C.S., Paltenghi, M., Le Tian, J., Pradel, M., Zhang, L.: Fuzz4all: Universal fuzzing with large language models. In: Proceedings of the IEEE/ACM 46th International Conference on Software Engineering (ICSE) (2024). <https://doi.org/10.1145/3597503.3639121>, <https://doi.org/10.1145/3597503.3639121>

56. Xu, M., Li, Z., Padon, O., Lin, S., Pointing, J., Hirth, A., Ma, H., Palsberg, J., Aiken, A., Acar, U.A., Jia, Z.: Quartz: superoptimization of quantum circuits. In: Proceedings of the 43rd ACM SIGPLAN International Conference on Programming Language Design and Implementation. p. 625–640. PLDI 2022, Association for Computing Machinery, New York, NY, USA (2022). <https://doi.org/10.1145/3519939.3523433>, <https://doi.org/10.1145/3519939.3523433>

A Additional PQASM Semantics and Typing Rules

$$\begin{array}{c}
\text{S-SEQC} \\
\frac{(\Phi, e_1) \xrightarrow{r} (\Phi', e'_1)}{(\Phi, e_1 ; e_2) \xrightarrow{r} (\Phi', e'_1 ; e_2)} \\
\\
\text{S-SEQT} \\
(\Phi, \{ \} ; e_2) \xrightarrow{1} (\Phi, e_2) \\
\\
\text{S-IFT} \\
(\Phi, \text{if } (\text{true}) e_1 \text{ else } e_2) \xrightarrow{1} (\Phi, e_1) \\
\\
\text{S-IFF} \\
(\Phi, \text{if } (\text{false}) e_1 \text{ else } e_2) \xrightarrow{1} (\Phi, e_2)
\end{array}$$

Fig. 17: Remaining program Level PQASM rules.

$$\begin{array}{c}
\text{SEQ} \\
\frac{\Omega \vdash_g \iota_1 \triangleright \Omega' \quad \Omega' \vdash_g \iota_2 \triangleright \Omega''}{\Omega \vdash_g \iota_1 ; \iota_2 \triangleright \Omega''} \\
\\
\text{ESEQ} \\
\frac{\Sigma ; \Omega \vdash e_1 \triangleright \Omega' \quad \Sigma ; \Omega' \vdash e_2 \triangleright \Omega''}{\Sigma ; \Omega \vdash e_1 ; e_2 \triangleright \Omega''} \\
\\
\text{TIF} \\
\frac{\Sigma \vdash B \quad \Sigma ; \Omega \vdash e_1 \triangleright \Omega' \quad \Sigma ; \Omega \vdash e_2 \triangleright \Omega'}{\Sigma ; \Omega \vdash \text{if } (B) e_1 \text{ else } e_2 \triangleright \Omega'}
\end{array}$$

Fig. 18: Remaining typing rules.

Figure 17 shows additional program-level semantic rules. Rules S-IFT and S-IFF perform classical conditional evaluation. In PQASM, the classical variables are evaluated via a substitution-based approach, as in S-MEA.

Figure 24 shows additional typing rules. In our type system, rule TIF ensures that any variables mentioned in B are properly scoped by the constraint $FV(B) \subseteq \Sigma$ ⁵, i.e., all free variables in B are bounded by Σ . Note that the two branches of TIF have the same output Σ' , i.e., the qubit manipulations in the two branches need to have the same effect. If one branch has a measurement on a qubit, the other branch must have the same qubit measurement.

B Additional Rules for Translation from Pqasm to SQIR

Figure 19 shows additional rules, which are the program-level rules, that translate a PQASM program to a hybrid Rocq program including SQIR circuits with possible measurement operations. Rule CNEXT connects the instruction and the

⁵ The rule is parameterized by different B formalism.

$$\begin{array}{c}
 \text{CRY} \\
 \frac{}{\Xi \vdash \text{Ry}^r q \gg (\gamma, \text{Ry}^r(\Xi(q)))} \\
 \\
 \text{CNEXT} \\
 \frac{\Xi \vdash \iota \gg \epsilon}{(n, \Xi, \iota) \gg (n, \Xi, \epsilon)} \\
 \\
 \text{CSEQ} \\
 \frac{(n, \Xi, e_1) \gg (n', \Xi', \chi_1) \quad (n', \Xi', e_2) \gg (n'', \Xi'', \chi_2)}{(n, \Xi, e_1 ; e_2) \rightarrow (n'', \Xi'', \chi_1 ; \chi_2)} \\
 \\
 \text{CNEW} \\
 \frac{\Xi' = \Xi[\forall q \in \bar{q}. q \mapsto |\Xi| + \text{ind}(\bar{q}, q)]}{(n, \Xi, \text{new}(\bar{q})) \gg (n + |\bar{q}|, \Xi', \{\})} \\
 \\
 \text{CMEA} \\
 \frac{(n, \Xi \setminus \bar{q}, e) \gg (n', \Xi', \chi)}{(n, \Xi, \text{let } x = \mathcal{M}(\bar{q}) \text{ in } e) \rightarrow (n', \Xi', \mathcal{M}(\bar{q}); \chi)} \\
 \\
 \text{CCU} \\
 \frac{\Xi \vdash \iota \gg \epsilon \quad \epsilon' = \text{ctrl}(\gamma(q), \epsilon)}{\Xi \vdash \text{CU } p \iota \gg \epsilon'} \\
 \\
 \text{CHAD} \\
 (n, \Xi, \mathbb{H}(q)) \gg (n, \Xi, \mathbb{H}(\Xi(q)))
 \end{array}$$

Fig. 19: Select PQASM to SQIR translation rules (SQIR circuits are marked blue). $|\Xi|$: the length of Ξ ; $\text{ind}(\bar{q}, q)$: the index of q in array \bar{q} . $\mathcal{M}(\bar{q})$ repeats $|\bar{q}|$ times on measuring qubit array \bar{q} .

program-level translations. Rule CHAD translates a Hadamard operation to a SQIR Hadamard gate, while rule CSEQ translates a sequencing operator.

Rule CNEW is one of the program-level rules, translating a qubit creation operation in PQASM. In SQIR, there is no qubit creation, in the sense that every qubit is assumed to exist in the first place. The translation essentially translates the operation to a SKIP operation in SQIR and increments the qubit heap size in the generated SQIR program. Note that the qubit size in the translation is always incrementing, i.e., a quantum measurement does not remove qubits but just makes some qubits inaccessible. Rule CMEA translates a PQASM measurement operation to SQIR measurements by repeatedly measuring out qubits in \bar{q} . The translation removes measured qubits from Ξ , but it does not modify the qubit size.

C OQASM: An Assembly Language for Quantum Oracles

The OQASM expression μ used in Figure 4 places an additional wrapper on top of the OQASM expression ι given in Figure 22. Here, we first provide a step-by-step explanation of OQASM.

OQASM is designed to express efficient quantum oracles that can be easily tested and, if desired, proved correct. OQASM operations leverage both the standard computational basis and an alternative basis connected by the quantum

Fourier transform (QFT). OQASM’s type system tracks the bases of variables in OQASM programs, forbidding operations that would introduce entanglement. OQASM states are therefore efficiently represented, so programs can be effectively tested and are simpler to verify and analyze. In addition, OQASM uses *virtual qubits* to support *position shifting operations*, which support arithmetic operations without introducing extra gates during translation. All of these features are novel to quantum assembly languages.

This section presents OQASM states and the language’s syntax, semantics, typing, and soundness results. As a running example, the QFT adder [11] is shown in Figure 20. The Rocq function `rz_adder` generates an OQASM program that adds two natural numbers `a` and `b`, each of length `n` qubits.

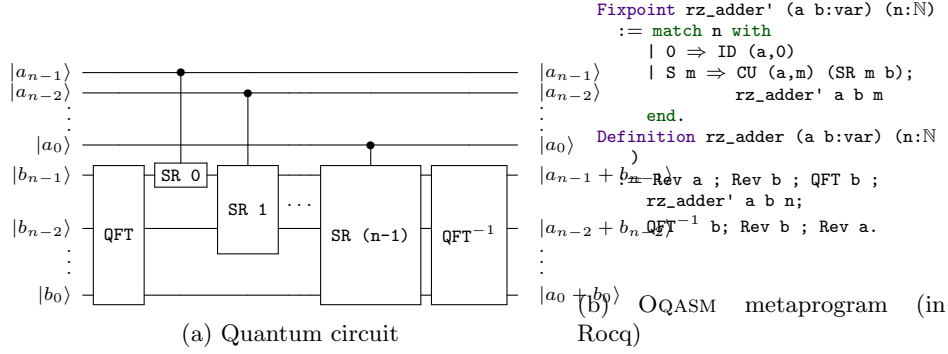


Fig. 20: Example OQASM program: QFT-based adder

C.1 OQASM States

Bit	$b ::= 0 \mid 1$
Natural number	$n \in \mathbb{N}$
Real	$r \in \mathbb{R}$
Phase	$\alpha(r) ::= e^{2\pi i r}$
Basis	$\tau ::= \text{Nor} \mid \text{Phi } n$
Unphased qubit	$\bar{q} ::= b\rangle \mid \Delta(r)\rangle$
Qubit	$q ::= \alpha(r)\bar{q}$
State (length d)	$\varphi ::= q_1 \otimes q_2 \otimes \dots \otimes q_d$

Fig. 21: OQASM state syntax

An OQASM program state is represented according to the grammar in Figure 21. A state φ of d qubits is a length- d tuple of qubit values q ; the state models the

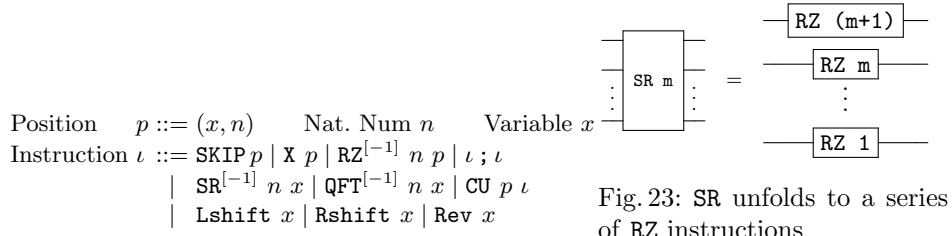


Fig. 23: SR unfolds to a series of RZ instructions

Fig. 22: OQASM syntax. For an operator OP , $\text{OP}^{[-1]}$ indicates that the operator has a built-in inverse available.

tensor product of those values. This means that the size of φ is $O(d)$ where d is the number of qubits. A d -qubit state in a language like SQIR is represented as a length 2^d vector of complex numbers, $O(2^d)$ in the number of qubits. Our linear state representation is possible because applying for any well-typed OQASM program on any well-formed OQASM state never causes qubits to be entangled.

A qubit value q has one of two forms \bar{q} , scaled by a global phase $\alpha(r)$. The two forms depend on the *basis* τ that the qubit is in—it could be either **Nor** or **Phi**. A **Nor** qubit has form $|b\rangle$ (where $b \in \{0, 1\}$), which is a computational basis value. A **Phi** qubit has the form $|\Delta(r)\rangle = \frac{1}{\sqrt{2}}(|0\rangle + \alpha(r)|1\rangle)$, which is a value of the (A)QFT basis. The number n in **Phi** n indicates the precision of the state φ . As shown by Beauregard [11], arithmetic on the computational basis can sometimes be more efficiently carried out on the QFT basis, which leads to the use of quantum operations (like QFT) when implementing circuits with classical input/output behavior.

C.2 OQASM Syntax, Typing, and Semantics

Figure 22 presents OQASM’s syntax. An OQASM program consists of a sequence of instructions ι . Each instruction applies an operator to either a variable x , representing a group of qubits, or a *position* p , which identifies a particular offset into a variable x .

The instructions in the first row correspond to simple single-qubit quantum gates—**SKIP** p , **X** p , and $\text{RZ}^{[-1]} n p$ —and instruction sequencing. The instructions in the next row apply to whole variables: **QFT** $n x$ applies the AQFT to variable x with n -bit precision and $\text{QFT}^{-1} n x$ applies its inverse. If n equals the size of x , then the AQFT operation is exact. $\text{SR}^{[-1]} n x$ applies a series of RZ gates (Figure 23). Operation **CU** $p \iota$ applies instruction ι *controlled* on qubit position p . All of the operations in this row—**SR**, **QFT**, and **CU**—will be translated to multiple SQIR gates. The function `rz_adder` in Figure 20(b) uses many of these instructions; e.g., it uses **QFT** and QFT^{-1} and applies **CU** to the m th position of variable **a** to control instruction **SR** m **b**.

$$\begin{array}{c}
\text{X} \\
\frac{\Omega(x) = \text{Nor} \quad n < \Sigma(x)}{\Sigma; \Omega \vdash \text{X}(x, n) \triangleright \Omega} \\
\\
\text{RZ} \qquad \text{SR} \\
\frac{\Omega(x) = \text{Nor} \quad n < \Sigma(x)}{\Sigma; \Omega \vdash \text{RZ } q(x, n) \triangleright \Omega} \qquad \frac{\Omega(x) = \text{Phi } n \quad m < n}{\Sigma; \Omega \vdash \text{SR } m \ x \triangleright \Omega} \\
\\
\text{QFT} \\
\frac{\Omega(x) = \text{Nor} \quad n \leq \Sigma(x)}{\Sigma; \Omega \vdash \text{QFT } n \ x \triangleright \Omega[x \mapsto \text{Phi } n]} \\
\\
\text{RQFT} \\
\frac{\Omega(x) = \text{Phi } n \quad n \leq \Sigma(x)}{\Sigma; \Omega \vdash \text{QFT}^{-1} n \ x \triangleright \Omega[x \mapsto \text{Nor}]} \\
\\
\text{CU} \qquad \text{LSH} \\
\frac{\Omega(x) = \text{Nor} \quad \text{fresh}(x, n) \ \iota \quad \text{neutral}(\iota)}{\Sigma; \Omega \vdash \iota \triangleright \Omega} \qquad \frac{\Omega(x) = \text{Nor}}{\Sigma; \Omega \vdash \text{Lshift } x \triangleright \Omega} \\
\\
\text{SEQ} \\
\frac{\Sigma; \Omega \vdash \iota_1 \triangleright \Omega' \quad \Sigma; \Omega' \vdash \iota_2 \triangleright \Omega''}{\Sigma; \Omega \vdash \iota_1 ; \iota_2 \triangleright \Omega''}
\end{array}$$

Fig. 24: Select OQASM typing rules

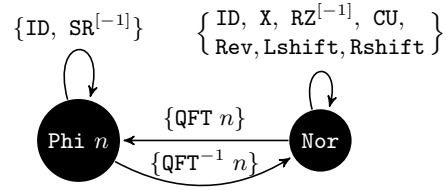


Fig. 25: Type rules' state machine

In the last row of Figure 22, instructions `Lshift` x , `Rshift` x , and `Rev` x are *position shifting operations*. Assuming that x has d qubits and x_k represents the k -th qubit state in x , `Lshift` x changes the k -th qubit state to $x_{(k+1)\%d}$, `Rshift` x changes it to $x_{(k+d-1)\%d}$, and `Rev` changes it to x_{d-1-k} . In our implementation, shifting is *virtual*, not physical. The OQASM translator maintains a logical map of variables/positions to concrete qubits and ensures that shifting operations are no-ops, introducing no extra gates.

Other quantum operations could be added to OQASM to allow reasoning about a larger class of quantum programs while still guaranteeing a lack of entanglement.

Typing In OQASM, typing is concerning a *type environment* Ω and a predefined *size environment* Σ , which map OQASM variables to their basis and size (number of qubits), respectively. The typing judgment is written $\Sigma; \Omega \vdash \iota \triangleright \Omega'$ which states that ι is well-typed under Ω and Σ , and transforms the variables' bases to be as in Ω' (Σ is unchanged). Σ is fixed because the number of qubits in execution is always fixed. It is generated in the high-level language compiler, such as `QIMP` in [32]. The algorithm generates Σ by taking an `QIMP` program and scanning through all the variable initialization statements. Select type rules are given in Figure 24; the rules not shown (for `ID`, `Rshift`, `Rev`, `RZ`⁻¹, and `SR`⁻¹) are similar.

The type system enforces three invariants. First, it enforces that instructions are well-formed, meaning that gates are applied to valid qubit positions (the

$\llbracket \text{SKIP } p \rrbracket \varphi$	$= \varphi$	
$\llbracket \text{X } (x, i) \rrbracket \varphi$	$= \varphi[(x, i) \mapsto \uparrow \text{xg}(\downarrow \varphi(x, i))]$	where $\text{xg}(0\rangle) = 1\rangle$ $\text{xg}(1\rangle) = 0\rangle$
$\llbracket \text{CU } (x, i) \ \iota \rrbracket \varphi$	$= \text{cu}(\downarrow \varphi(x, i), \iota, \varphi)$	where $\text{cu}(0\rangle, \iota, \varphi) = \varphi$ $\text{cu}(1\rangle, \iota, \varphi) = \llbracket \iota \rrbracket \varphi$
$\llbracket \text{RZ } m \ (x, i) \rrbracket \varphi$	$= \varphi[(x, i) \mapsto \uparrow \text{rz}(m, \downarrow \varphi(x, i))]$	where $\text{rz}(m, 0\rangle) = 0\rangle$ $\text{rz}(m, 1\rangle) = \alpha(\frac{1}{2^m}) 1\rangle$
$\llbracket \text{RZ}^{-1} \ m \ (x, i) \rrbracket \varphi$	$= \varphi[(x, i) \mapsto \uparrow \text{rrz}(m, \downarrow \varphi(x, i))]$	where $\text{rrz}(m, 0\rangle) = 0\rangle$ $\text{rrz}(m, 1\rangle) = \alpha(-\frac{1}{2^m}) 1\rangle$
$\llbracket \text{SR } m \ x \rrbracket \varphi$	$= \varphi[\forall i \leq m. (x, i) \mapsto \uparrow \Delta(r_i + \frac{1}{2^{m-i+1}})]$	when $\downarrow \varphi(x, i) = \Delta(r_i)\rangle$
$\llbracket \text{SR}^{-1} \ m \ x \rrbracket \varphi$	$= \varphi[\forall i \leq m. (x, i) \mapsto \uparrow \Delta(r_i - \frac{1}{2^{m-i+1}})]$	when $\downarrow \varphi(x, i) = \Delta(r_i)\rangle$
$\llbracket \text{QFT } n \ x \rrbracket \varphi$	$= \varphi[x \mapsto \uparrow \text{qt}(\Sigma(x), \downarrow \varphi(x), n)]$	where $\text{qt}(i, y\rangle, n) = \bigotimes_{k=0}^{i-1} (\Delta(\frac{y}{2^{n-k}})\rangle)$
$\llbracket \text{QFT}^{-1} \ n \ x \rrbracket \varphi$	$= \varphi[x \mapsto \uparrow \text{qt}^{-1}(\Sigma(x), \downarrow \varphi(x), n)]$	
$\llbracket \text{Lshift } x \rrbracket \varphi$	$= \varphi[x \mapsto \text{pm}_l(\varphi(x))]$	where $\text{pm}_l(q_0 \otimes q_1 \otimes \dots \otimes q_{n-1}) = q_{n-1} \otimes q_0 \otimes q_1 \otimes \dots$
$\llbracket \text{Rshift } x \rrbracket \varphi$	$= \varphi[x \mapsto \text{pm}_r(\varphi(x))]$	where $\text{pm}_r(q_0 \otimes q_1 \otimes \dots \otimes q_{n-1}) = q_1 \otimes \dots \otimes q_{n-1} \otimes q_0$
$\llbracket \text{Rev } x \rrbracket \varphi$	$= \varphi[x \mapsto \text{pm}_a(\varphi(x))]$	where $\text{pm}_a(q_0 \otimes \dots \otimes q_{n-1}) = q_{n-1} \otimes \dots \otimes q_0$
$\llbracket \iota_1 ; \iota_2 \rrbracket \varphi$	$= \llbracket \iota_2 \rrbracket (\llbracket \iota_1 \rrbracket \varphi)$	

$$\begin{aligned}
 & \downarrow \alpha(b)\bar{q} = \bar{q} \quad \downarrow (q_1 \otimes \dots \otimes q_n) = \downarrow q_1 \otimes \dots \otimes \downarrow q_n \\
 & \varphi[(x, i) \mapsto \uparrow \bar{q}] = \varphi[(x, i) \mapsto \alpha(b)\bar{q}] \quad \textbf{where } \varphi(x, i) = \alpha(b)\bar{q}_i \\
 & \varphi[(x, i) \mapsto \uparrow \alpha(b_1)\bar{q}] = \varphi[(x, i) \mapsto \alpha(b_1 + b_2)\bar{q}] \quad \textbf{where } \varphi(x, i) = \alpha(b_2)\bar{q}_i \\
 & \varphi[x \mapsto q_x] = \varphi[\forall i < \Sigma(x). (x, i) \mapsto q_{(x, i)}] \\
 & \varphi[x \mapsto \uparrow q_x] = \varphi[\forall i < \Sigma(x). (x, i) \mapsto \uparrow q_{(x, i)}]
 \end{aligned}$$

Fig. 26: OQASM semantics

second premise in X) and that any control qubit is distinct from the target(s) (the **fresh** premise in CU). This latter property enforces the quantum *no-cloning rule*. For example, applying the CU in **rz_adder'** (Figure 20) is valid because position **a,m** is distinct from variable **b**.

Second, the type system enforces that instructions leave affected qubits on a proper basis (thereby avoiding entanglement). The rules implement the state machine shown in Figure 25. For example, QFT n transforms a variable from **Nor** to **Phi** n (rule QFT), while QFT⁻¹ n transforms it from **Phi** n back to **Nor** (rule RQFT). Position shifting operations are disallowed on variables x in the **Phi** basis because the qubits that makeup x are internally related (see Definition 3) and cannot be rearranged. Indeed, applying a **Lshift** and then a QFT⁻¹ on x in **Phi** would entangle x 's qubits.

Third, the type system enforces that the effect of position-shifting operations can be statically tracked. The **neutral** condition of CU requires that any shifting within ι is restored by the time it completes. For example, CU p (**Lshift** x) ; X $(x, 0)$ is not well-typed because knowing the final physical position of qubit $(x, 0)$ would require statically knowing the value of p . On the other hand, the program CU c (**Lshift** x ; X $(x, 0)$) ; **Rshift** x) ; X $(x, 0)$ is well-typed because the effect of the **Lshift** is “undone” by an **Rshift** inside the body of the CU.

Semantics The semantics of an OQASM program is a partial function $\llbracket \cdot \rrbracket$ from an instruction ι and input state φ to an output state φ' , written $\llbracket \iota \rrbracket \varphi = \varphi'$, shown in Figure 26.

Recall that a state φ is a tuple of d qubit values, modeling the tensor product $q_1 \otimes \cdots \otimes q_d$. The rules implicitly map each variable x to a range of qubits in the state, e.g., $\varphi(x)$ corresponds to some sub-state $q_k \otimes \cdots \otimes q_{k+n-1}$ where $\Sigma(x) = n$. Many of the rules in Figure 26 update a *portion* of a state. $\varphi[(x, i) \mapsto q_{(x, i)}]$ updates the i -th qubit of variable x to be the (single-qubit) state $q_{(x, i)}$, and $\varphi[x \mapsto q_x]$ to update variable x according to the qubit *tuple* q_x . $\varphi[(x, i) \mapsto \uparrow q_{(x, i)}]$ and $\varphi[x \mapsto \uparrow q_x]$ are similar, except that they also accumulate the previous global phase of $\varphi(x, i)$ (or $\varphi(x)$). \downarrow is to convert a qubit $\alpha(b)\bar{q}$ to an unphased qubit \bar{q} .

Function **xg** updates the state of a single qubit according to the rules for the standard quantum gate X . **cu** is a conditional operation depending on the **Nor**-basis qubit (x, i) . **RZ** (or RZ^{-1}) is an z-axis phase rotation operation. Since it applies to **Nor**-basis, it applies a global phase. By Theorem 6, when it is compiled to SQIR, the global phase might be turned into a local one. For example, to prepare the state $\sum_{j=0}^{2^n-1} (-i)^x |x\rangle$ [18], a series of Hadamard gates are applied, followed by several controlled-RZ gates on x , where the controlled-RZ gates are definable by OQASM. **SR** (or SR^{-1}) applies an $m + 1$ series of RZ (or RZ^{-1}) rotations where the i -th rotation applies a phase of $\alpha(\frac{1}{2^{m-i+1}})$ (or $\alpha(-\frac{1}{2^{m-i+1}})$). **qt** applies an approximate quantum Fourier transform; $|y\rangle$ is an abbreviation of $|b_1\rangle \otimes \cdots \otimes |b_i\rangle$ (assuming $\Sigma(y) = i$) and n is the degree of approximation. If $n = i$, then the operation is the standard QFT. Otherwise, each qubit in the state is mapped to $|\Delta(\frac{y}{2^{n-k}})\rangle$, which is equal to $\frac{1}{\sqrt{2}}(|0\rangle + \alpha(\frac{y}{2^{n-k}})|1\rangle)$ when $k < n$ and $\frac{1}{\sqrt{2}}(|0\rangle + |1\rangle) = |+\rangle$ when $n \leq k$ (since $\alpha(n) = 1$ for any natural number n). qt^{-1} is the inverse function of **qt**. Note that the input state to qt^{-1} is guaranteed to have the form $\bigotimes_{k=0}^{i-1} (|\Delta(\frac{y}{2^{n-k}})\rangle)$ because it has type **Phi** n . pm_l , pm_r , and pm_a are the semantics for **Lshift**, **Rshift**, and **Rev**, respectively.

C.3 OQASM Metatheory

Soundness The following statement is proved: well-typed OQASM programs are well-defined; i.e., the type system is sound concerning the semantics. Below is the well-formedness of an OQASM state.

Definition 3 (Well-formed Oqasm state). A state φ is *well-formed*, written $\Sigma; \Omega \vdash \varphi$, iff:

- For every $x \in \Omega$ such that $\Omega(x) = \text{Nor}$, for every $k < \Sigma(x)$, $\varphi(x, k)$ has the form $\alpha(r)|b\rangle$.
- For every $x \in \Omega$ such that $\Omega(x) = \text{Phi } n$ and $n \leq \Sigma(x)$, there exists a value v such that for every $k < \Sigma(x)$, $\varphi(x, k)$ has the form $\alpha(r)|\Delta(\frac{v}{2^{n-k}})\rangle$.⁶

Type soundness is stated as follows; the proof is by induction on ι and is mechanized in Rocq.

⁶ Note that $\Phi(x) = \Phi(x + n)$, where the integer n refers to phase $2\pi n$; so multiple choices of v are possible.

Theorem 4. [OQASM type soundness] If $\Sigma; \Omega \vdash \iota \triangleright \Omega'$ and $\Sigma; \Omega \vdash \varphi$ then there exists φ' such that $\llbracket \iota \rrbracket \varphi = \varphi'$ and $\Sigma; \Omega' \vdash \varphi'$.

Algebra Mathematically, the set of well-formed d -qubit OQASM states for a given Ω can be interpreted as a subset \mathcal{S}^d of a 2^d -dimensional Hilbert space \mathcal{H}^d ⁷. The semantics function $\llbracket \cdot \rrbracket$ can be interpreted as a $2^d \times 2^d$ unitary matrix, as is standard when representing the semantics of programs without measurement [27]. Because OQASM's semantics can be viewed as a unitary matrix, correctness properties extend by linearity from \mathcal{S}^d to \mathcal{H}^d —an oracle that performs addition for classical `Nor` inputs will also perform addition over a superposition of `Nor` inputs. The following statement is proved: \mathcal{S}^d is closed under well-typed OQASM programs.

Given a qubit size map Σ and type environment Ω , the set of OQASM programs that are well-typed concerning Σ and Ω (i.e., $\Sigma; \Omega \vdash \iota \triangleright \Omega'$) form an algebraic structure $(\{\iota\}, \Sigma, \Omega, \mathcal{S}^d)$, where $\{\iota\}$ defines the set of valid program syntax, such that there exists $\Omega', \Sigma; \Omega \vdash \iota \triangleright \Omega'$ for all ι in $\{\iota\}$; \mathcal{S}^d is the set of d -qubit states on which programs $\iota \in \{\iota\}$ are run, and are well-formed ($\Sigma; \Omega \vdash \varphi$) according to Definition 3. From the OQASM semantics and the type soundness theorem, for all $\iota \in \{\iota\}$ and $\varphi \in \mathcal{S}^d$, such that $\Sigma; \Omega \vdash \iota \triangleright \Omega'$ and $\Sigma; \Omega \vdash \varphi$, and $\llbracket \iota \rrbracket \varphi = \varphi', \Sigma; \Omega' \vdash \varphi'$, and $\varphi' \in \mathcal{S}^d$. Thus, $(\{\iota\}, \Sigma, \Omega, \mathcal{S}^d)$, where $\{\iota\}$ defines a groupoid.

The groupoid can be certainly extended to another algebraic structure $(\{\iota'\}, \Sigma, \mathcal{H}^d)$, where \mathcal{H}^d is a general 2^d dimensional Hilbert space \mathcal{H}^d and $\{\iota'\}$ is a universal set of quantum gate operations. Clearly, the following is true: $\mathcal{S}^d \subseteq \mathcal{H}^d$ and $\{\iota\} \subseteq \{\iota'\}$, because sets \mathcal{H}^d and $\{\iota'\}$ can be acquired by removing the well-formed ($\Sigma; \Omega \vdash \varphi$) and well-typed ($\Sigma; \Omega \vdash \iota \triangleright \Omega'$) definitions for \mathcal{S}^d and $\{\iota\}$, respectively. $(\{\iota'\}, \Sigma, \mathcal{H}^d)$ is a groupoid because every OQASM operation is valid in a traditional quantum language like SQIR. The following two theorems are to connect OQASM operations with operations in the general Hilbert space:

Theorem 5. $(\{\iota\}, \Sigma, \Omega, \mathcal{S}^d) \subseteq (\{\iota'\}, \Sigma, \mathcal{H}^d)$ is a subgroupoid.

Theorem 6. Let $|y\rangle$ be an abbreviation of $\bigotimes_{m=0}^{d-1} \alpha(r_m) |b_m\rangle$ for $b_m \in \{0, 1\}$. If for every $i \in [0, 2^d)$, $\llbracket \iota \rrbracket |y_i\rangle = |y'_i\rangle$, then $\llbracket \iota \rrbracket (\sum_{i=0}^{2^d-1} |y_i\rangle) = \sum_{i=0}^{2^d-1} |y'_i\rangle$.

The following theorems are proved as corollaries of the compilation correctness theorem from OQASM to SQIR ([32]). Theorem 5 suggests that the space \mathcal{S}^d is closed under the application of any well-typed OQASM operation. Theorem 6 says that OQASM oracles can be safely applied to superpositions over classical states.⁸

⁷ A *Hilbert space* is a vector space with an inner product that is complete with respect to the norm defined by the inner product. \mathcal{S}^d is a *subset*, not a *subspace* of \mathcal{H}^d because \mathcal{S}^d is not closed under addition: Adding two well-formed states can produce a state that is not well-formed.

⁸ Note that a superposition over classical states can describe *any* quantum state, including entangled states.

$$\begin{array}{l}
 X(x, n) \xrightarrow{\text{inv}} X(x, n) \qquad SR\ m\ x \xrightarrow{\text{inv}} SR^{-1}\ m\ x \qquad QFT\ n\ x \xrightarrow{\text{inv}} QFT^{-1}\ n\ x \\
 Lshift\ x \xrightarrow{\text{inv}} Rshift\ x \qquad \frac{\iota \xrightarrow{\text{inv}} \iota'}{CU(x, n)\ \iota \xrightarrow{\text{inv}} CU(x, n)\ \iota'} \qquad \frac{\iota_1 \xrightarrow{\text{inv}} \iota'_1 \quad \iota_2 \xrightarrow{\text{inv}} \iota'_2}{\iota_1 ; \iota_2 \xrightarrow{\text{inv}} \iota'_2 ; \iota'_1}
 \end{array}$$

Fig. 27: Select OQASM inversion rules

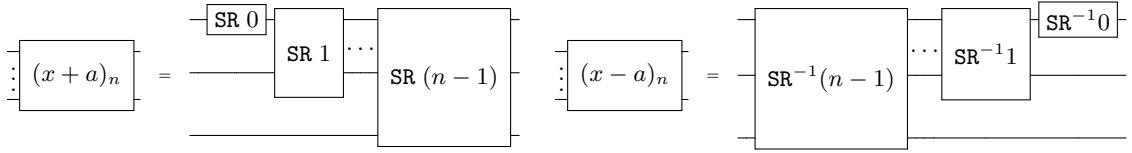


Fig. 28: Addition/subtraction circuits are inverses

OQASM programs are easily invertible, as shown by the rules in Figure 27. This inversion operation is useful for constructing quantum oracles; for example, the core logic in the QFT-based subtraction circuit is just the inverse of the core logic in the addition circuit (Figure 27). This allows us to reuse the proof of addition in the proof of subtraction. The inversion function satisfies the following properties:

Theorem 7. [Type reversibility] For any well-typed program ι , such that $\Sigma; \Omega \vdash \iota \triangleright \Omega'$, its inverse ι' , where $\iota \xrightarrow{\text{inv}} \iota'$, is also well-typed and $\Sigma; \Omega' \vdash \iota' \triangleright \Omega$. Moreover, $\llbracket \iota; \iota' \rrbracket \varphi = \varphi$.